

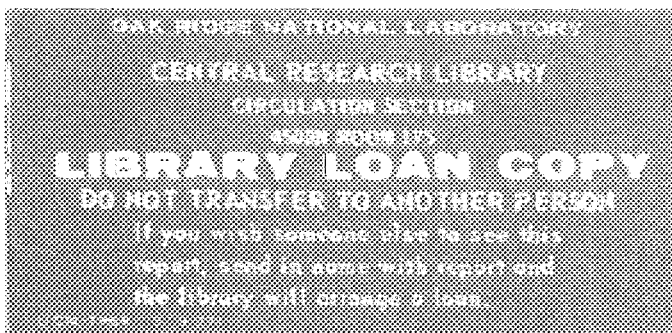
ORNL/TM-10836

**OAK RIDGE  
NATIONAL  
LABORATORY**

**MARTIN MARIETTA**

**Pilot-Scale Demonstration of  
Process Wastewater Decontamination  
Using Chabazite Zeolites**

S. M. Robinson  
J. R. Parrott, Jr.



OPERATED BY  
MARTIN MARIETTA ENERGY SYSTEMS, INC.  
FOR THE UNITED STATES  
DEPARTMENT OF ENERGY



Chemical Technology Division

ORNL Waste Management Operations Program  
(Activity No. GF 01 02 06 0, ONL-WN01)

PILOT-SCALE DEMONSTRATION OF PROCESS WASTEWATER DECONTAMINATION  
USING CHABAZITE ZEOLITES

S. M. Robinson  
J. R. Parrott, Jr.

Engineering Development Section

Date Published - December 1989

Prepared by the  
OAK RIDGE NATIONAL LABORATORY  
Oak Ridge, Tennessee 37831  
operated by  
MARTIN MARIETTA ENERGY SYSTEMS, INC.  
for the  
U.S. DEPARTMENT OF ENERGY  
under contract No. DE-AC05-84OR21400

MARTIN MARIETTA ENERGY SYSTEMS LIBRARIES



3 4456 0328842 1



## CONTENTS

LIST OF FIGURES . . . . .	iv
LIST OF TABLES . . . . .	v
LIST OF SYMBOLS . . . . .	vi
ABSTRACT . . . . .	1
EXECUTIVE SUMMARY . . . . .	2
1. INTRODUCTION . . . . .	6
2. BACKGROUND . . . . .	12
3. EXPERIMENTAL RESULTS . . . . .	20
3.1 NEAR-FULL-SCALE COLUMNS FOR $^{137}\text{Cs}$ DECONTAMINATION . . . . .	20
3.2 PILOT-SCALE COLUMNS FOR $^{90}\text{Sr}$ AND $^{137}\text{Cs}$ DECONTAMINATION . . . . .	25
4. MODELING OF EXPERIMENTAL RESULTS . . . . .	34
5. ECONOMIC ANALYSES . . . . .	41
6. CONCLUSIONS AND RECOMMENDATIONS . . . . .	46
7. REFERENCES . . . . .	48
8. APPENDIX . . . . .	50
8.1 APPENDIX A. EXPERIMENTAL DATA . . . . .	50
8.2 APPENDIX B. MODEL DEVELOPMENT . . . . .	63

## LIST OF FIGURES

<u>Figure</u>		<u>Page</u>
1	Decontamination flowsheet for the Process Waste Treatment Plant . . . . .	10
2	Proposed decontamination flowsheet for the Process Waste Treatment Plant . . . . .	11
3	Schematic of 3.7-m <sup>3</sup> pressure vessel demineralizers used in near-full-scale Ionsiv IE-95 zeolite tests . .	13
4	Breakthrough data for near-full-scale test with Ionsiv IE-95 for <sup>90</sup> Sr removal from process wastewater . . . . .	14
5	Schematic of 0.57-m <sup>3</sup> pressure vessel demineralizers used in pilot-scale TSM-300 zeolite tests . . . . .	16
6	Breakthrough data for pilot-scale test with TSM-300 zeolite for <sup>90</sup> Sr removal from process wastewater with zeolite prefilter . . . . .	18
7	<sup>137</sup> Cs effluent concentration from near-full-scale Ionsiv IE-95 columns for treatment of process wastewater . . . . .	22
8	Residence times for near-full-scale columns containing Ionsiv IE-95 zeolite . . . . .	24
9	Breakthrough data for first column in pilot-scale test with TSM-300 zeolite for <sup>90</sup> Sr removal from process wastewater . . . . .	28
10	<sup>90</sup> Sr effluent concentrations from TSM-300 pilot-scale test for treatment of process wastewater . . . .	29
11	Modeled breakthrough curve for near-full-scale test with Ionsiv IE-95 for <sup>137</sup> Cs removal from process wastewater . . . . .	36
12	Modeled breakthrough curve for pilot-scale test with TSM-300 zeolite for <sup>90</sup> Sr removal from process wastewater . . . . .	37

LIST OF TABLES

<u>Table</u>		<u>Page</u>
1	Typical composition of ORNL's process wastewater . . .	7
2	Predicted values of N for scaleup of <sup>90</sup> Sr laboratory data . . . . .	38
3	Comparison of alternative flowsheets for PWTP upgrade . . . . .	42
A.1	Breakthrough data for near-full-scale zeolite column . . . . .	51
A.2	Breakthrough data for pilot-scale zeolite columns . . .	57
A.3	Pressure drops across pilot-scale zeolite columns . . .	60

## LIST OF SYMBOLS

$a$	=	coefficient for Eq. 14.
$A$	=	concentration of cation reacting, g-mol/cm <sup>3</sup> .
$B$	=	concentration of cation reacting, g-mol/cm <sup>3</sup> .
$C$	=	concentration of solute in effluent, g-mol/cm <sup>3</sup> .
$C_0$	=	concentration of solute in feed, g-mol/cm <sup>3</sup> .
$d$	=	particle diameter, cm.
$D$	=	diffusion coefficient.
$f$	=	flow rate through column, cm <sup>3</sup> /s.
$k_f$	=	film-diffusion-rate coefficient.
$k_p$	=	solid-diffusion-rate coefficient.
$K_a$	=	mass-transfer coefficient, l/s.
$K_d$	=	distribution coefficient, dimensionless.
$K'_d$	=	distribution coefficient, cm <sup>3</sup> /g.
$N$	=	number of mass-transfer units, dimensionless.
$S$	=	cross-sectional area of column, cm.
$q$	=	concentration of solute in solid, g-mol/g.
$q^*$	=	concentration of solute in solid at equilibrium, g-mol/g.
$q_v$	=	concentration of solute per unit volume of sorbent bed, g-mol/g.
$R$	=	separation factor, dimensionless.
$T$	=	throughput parameter, dimensionless.
$V$	=	effluent volume, cm <sup>3</sup> .
$v$	=	sorbent bed volume, cm <sup>3</sup> .
$X$	=	concentration of solute in fluid phase, dimensionless.
$Y$	=	concentration of solute in solid phase, dimensionless.

### Greek Letters

$\rho_b$	=	bulk density of sorbent, g/cm <sup>3</sup> .
----------	---	--

PILOT-SCALE DEMONSTRATION OF PROCESS WASTEWATER  
DECONTAMINATION USING CHABAZITE ZEOLITES

S. M. Robinson  
J. R. Parrott, Jr.

ABSTRACT

Improved precipitation and ion-exchange methods are being developed to decontaminate Oak Ridge National Laboratory (ORNL) process wastewaters containing small amounts of  $^{90}\text{Sr}$  and  $^{137}\text{Cs}$  while minimizing waste generation. A wide range of potential processes have been tested in laboratory-scale scouting tests. Based on the data from these scouting tests, several alternative flowsheets have been developed for long-term upgrade of the facility. The primary objective of these proposed flowsheets is to minimize secondary waste generation, particularly liquid wastes, and produce a nonhazardous waste form that can be safely stored with minimum surveillance.

The most promising process consists of passing wastewater through a series of columns containing chabazite zeolite, an inorganic ion-exchange material, to remove both cesium and strontium. The flowsheet has the advantage of being a simple, reliable process that produces one type of solid waste. The feasibility of this process has been demonstrated using pilot-scale equipment at the Process Waste Treatment Plant (PWTP). A single near-full-scale column has also been tested at the PWTP for cesium removal. This report summarizes the results of both chabazite tests performed at the PWTP in 1987.

## EXECUTIVE SUMMARY

Improved chemical precipitation and/or ion-exchange methods are being developed at the Oak Ridge National Laboratory (ORNL) in an effort to reduce waste generation at the Process Waste Treatment Plant (PWTP). A wide variety of screening tests were performed on potential precipitation techniques and ion-exchange materials on a laboratory scale. The results from these bench-scale tests were used to determine the optimal combination of processes for potential flowsheets for possible installation at the PWTP. Two flowsheets were selected for further testing; both flowsheets contained chabazite zeolite ion-exchange unit operations.

Results from the bench-scale tests indicated that the chabazite zeolites have extremely high sorption capacity for cesium in process wastewater. The chabazites have a much lower sorption capacity for strontium, but they had the highest sorption capacity of any material tested if the wastewater was not pretreated for removal of the nonradioactive ions which compete with strontium for sites on the ion-exchange material. Several materials, including the strong-acid ion-exchange resin presently used at the PWTP, have higher sorption capacities for strontium if the calcium and magnesium ions are removed prior to ion exchange.

The two flowsheets selected for additional testing are described in the following text. One flowsheet uses several chabazite zeolite columns in series to remove both  $^{90}\text{Sr}$  and  $^{137}\text{Cs}$ . The other flowsheet uses a single chabazite zeolite to remove  $^{137}\text{Cs}$ , a precipitator to remove calcium and magnesium, and HCR-S strong-acid resin to remove

$^{90}\text{Sr}$ . This report summarizes the results of large-scale testing of zeolite columns for (1) use of one column to remove  $^{137}\text{Cs}$  from the wastewater prior to additional unit operations to remove  $^{90}\text{Sr}$ , and (2) use of several columns in series to remove both  $^{137}\text{Cs}$  and  $^{90}\text{Sr}$ .

A 3.7- $\text{m}^3$  demineralizer pressure vessel (near-full-plant scale) containing Ionsiv IE-95, a synthetic chabazite produced by Union Carbide, was temporarily installed at the PWTP to remove cesium from the feedwater. The objective of this test was to verify modeling results obtained from the laboratory-scale tests and to determine if factors other than the sorption capacity of the zeolite would determine the life of the column. This column was in operation from February 2, 1987, to December 3, 1987, and processed 22,700 bed volumes (BVs) 22,500,000 gal of wastewater. The zeolite reduced the cesium concentration from 160 Bq/L to <45 Bq/L during this 10-month period. The effluent concentration was still well below the proposed limit of 111 Bq/L when the run was terminated due to column plugging.

This test successfully demonstrated the feasibility of using chabazites to remove  $^{137}\text{Cs}$  from ORNL process wastewater. The process is simple and reliable and only requires occasional backwashing (once every 1-2 months for this system). The backwashing operation was very cumbersome for this unit operation; however, proper design of permanent equipment could overcome the problems encountered during this test.

A series of four sluiceable pressure vessels containing TSM-300 (formerly PDZ-300), a natural chabazite distributed by Tenneco Speciality Minerals, was used to test removal of  $^{137}\text{Cs}$  and  $^{90}\text{Sr}$  at 10% plant scale from April to November 1987. These columns were operated

to demonstrate the feasibility of and develop techniques for operating columns in series, to verify the laboratory-scale modeling results, and to determine parameters which would be important in the design of full-scale equipment. The system was operated by removing the lead zeolite column from operation after 3000 BVs of wastewater were processed, replacing the loaded zeolite with fresh material, and moving the fresh column to the end of the train.

During the 7-month period of operation, 15,000 BVs (2,250,000 gal) of wastewater were treated and 6 BVs (900 gal) of spent zeolite were produced. The zeolites removed the  $^{137}\text{Cs}$  to below the detection limits during the entire run. The  $^{90}\text{Sr}$  effluent concentration from the system ranged between 1 and 30 Bq/L (the proposed limits for  $^{90}\text{Sr}$  discharge are 37 Bq/L). Since the pressure vessels used in these tests were not designed specifically for this application, some loaded zeolite remained in the columns during the sluicing/reloading process. The  $^{90}\text{Sr}$  effluent concentration could have been kept to <10 Bq/L using the same operating procedures, if the equipment had been properly designed for zeolite removal. The data also indicated that channeling and/or plugging were the limiting factor(s) for column life, not the zeolite sorption capacity.

This test successfully demonstrated the feasibility of using chabazite columns in series to remove both  $^{137}\text{Cs}$  and  $^{90}\text{Sr}$  from ORNL process wastewater. Although this test was performed using equipment that was not designed for the application and column plugging lowered the potential capacity of the system, analyses of the experimental data

indicate that the chabazite system would be more economical to operate than the existing PWTP flowsheet.

Several areas were identified in this study which need additional attention in order to optimize the zeolite operation. The design of the column will be a major factor in determining the efficiency of a zeolite system. The columns must be designed for complete removal of loaded zeolites from the ion-exchange column. The system must also be designed with adequate air-sparging and backwashing capabilities to assure long column life and minimize secondary waste generation. Additional studies are needed to determine the factors that cause column plugging. Posttreatment processes may be needed to reduce the leachability of zeolites that have been loaded with radionuclides.

The design of the columns is extremely important to efficiency of the zeolite system. However, the experimental data obtained in this study could not be accurately predicted from previous bench-scale data using traditional modeling techniques. Fundamental studies in multicomponent liquid ion exchange are needed to develop models that could be used to design columns for maximum efficiency, minimize secondary waste generation, and eliminate extensive pilot-scale testing in the future. This type of model could amount to significant cost savings for the PWTP design as well as any other waste stream requiring treatment by ion exchange. The cost savings will increase significantly as disposal costs for secondary waste increase.

## 1. INTRODUCTION

The process waste system at the Oak Ridge National Laboratory (ORNL) is used to collect waste streams that have the potential to be contaminated with radionuclides and water that is contaminated with very low levels of radioactivity, including groundwater and condensate from the liquid low-level waste evaporator. Each month, about  $5 \times 10^6$  gal of wastes are decontaminated at the Process Waste Treatment Plant (PWTP). A typical characterization of the process waste stream is shown in Table 1. The radionuclide composition of the feed varies widely; concentrations have been as high as 8000 Bq/L  $^{90}\text{Sr}$  and 1000 Bq/L  $^{137}\text{Cs}$ . The major chemical constituents (calcium, magnesium, and sodium bicarbonates) are introduced by contaminated groundwater.

Prior to 1986, decontamination of process wastewater was accomplished by filtration and ion exchange using HCR-S resin manufactured by the Dow Chemical Company.<sup>1</sup> These processes were easily operated and could accommodate the large fluctuations in feed-stream flow rates and compositions, which result from the multipurpose research facilities at ORNL. However, this decontamination process produced large amounts of secondary liquid wastes.

New regulations and higher costs for disposal of the concentrated secondary liquid wastes have prompted efforts to improve the efficiency of the PWTP. Since disposal by hydrofracture has been discontinued, an alternative means for disposing of contaminated liquid waste must be implemented. Currently, there is limited storage capacity in the Melton Valley Storage Tanks (which are being used to store the wastes

Table 1. Typical composition of ORNL's process wastewater

Radioactive components	Concentration (Bq/L)	Chemical components	Concentration (mg/L)	Chemical parameter	Concentration (mg/L)
Gross alpha	<30	Ca	40	pH	8.8
Gross beta	3500	Mg	10	TDS <sup>a</sup>	250
<sup>60</sup> Co	25	Na	20	TSS <sup>b</sup>	3
<sup>90</sup> Sr	2000	Sr	0.2	Total	133
<sup>95</sup> ZrNb	50	HCO <sub>3</sub>	60	Alkalinity	125
<sup>106</sup> Ru	10	SO <sub>4</sub>	18	COD <sup>c</sup>	6
<sup>137</sup> Cs	200	Cl	6	TOC <sup>d</sup>	12

<sup>a</sup>Total dissolved solids.

<sup>b</sup>Total suspended solids.

<sup>c</sup>Chemical oxygen demand.

<sup>d</sup>Total organic carbon.

until a new disposal method can be implemented). Alternative means for disposing of contaminated liquid wastes will also be more costly than disposal via hydrofracture. Therefore, efforts to reduce the generation of contaminated liquid wastes have been vigorously implemented at ORNL. Because the PWTP generated ~30 vol % and ~80 wt % of ORNL's contaminated liquid wastes in 1985,<sup>2</sup> it was targeted for upgrade.

In 1985-86, extensive research and development studies were conducted on potential improved treatment methods to support PWTP process improvements. Bench-scale precipitation and ion-exchange methods were tested to determine the optimal combination of processes.<sup>3,4</sup> The results from these scoping tests were used to develop the potential flowsheets for installation at the PWTP. These flowsheets were modeled to determine the operating conditions and to estimate waste generation at plant scale. The results were used to evaluate the potential of each flowsheet for installation at the PWTP.<sup>2,5</sup>

The evaluation indicated that the secondary waste generation rate could immediately be reduced by partial upgrade of the PWTP. In 1986, the PWTP was upgraded by installing a chemical precipitator at the head end of the PWTP to remove nonradioactive cations, primarily calcium and magnesium, prior to removal of <sup>90</sup>Sr by ion exchange. Under these conditions, the ion-exchange columns would no longer remove <sup>137</sup>Cs.

The PWTP feed presently meets cesium discharge limits without treatment. Currently, the PWTP effluent requirements for radionuclides are set by 10 CFR Pt. 20 at 11.1 Bq/L for <sup>90</sup>Sr and 740 Bq/L for <sup>137</sup>Cs.

However, DOE Order 5480.XX has proposed to change the discharge limits for  $^{90}\text{Sr}$  and  $^{137}\text{Cs}$  to 37 Bq/L and 111 Bq/L, respectively. Under these conditions, additional treatment for cesium removal would be required. Therefore, an experimental near-full-scale chabazite zeolite column was installed in front of the chemical precipitator for cesium removal in 1987. The treatment process presently used at the PWTP is shown in Fig. 1.

The flowsheet evaluation indicated that the most promising process for long-term upgrade of the PWTP consists of passing the water through a series of columns containing chabazite zeolites. This flowsheet (shown in Fig. 2) is being tested at the PWTP on a pilot scale using four columns. Similar systems are being developed to treat radioactive wastewaters at West Valley, New York;<sup>6</sup> Savannah River, South Carolina;<sup>7</sup> and in England.<sup>8</sup>

This report summarizes the results from the pilot-scale and near-full-scale zeolite column tests performed at the PWTP in 1987. The experimental results, modeling of the experimental data, and an economic analyses of both processes are included.

ORNL DWG 86-1029R3

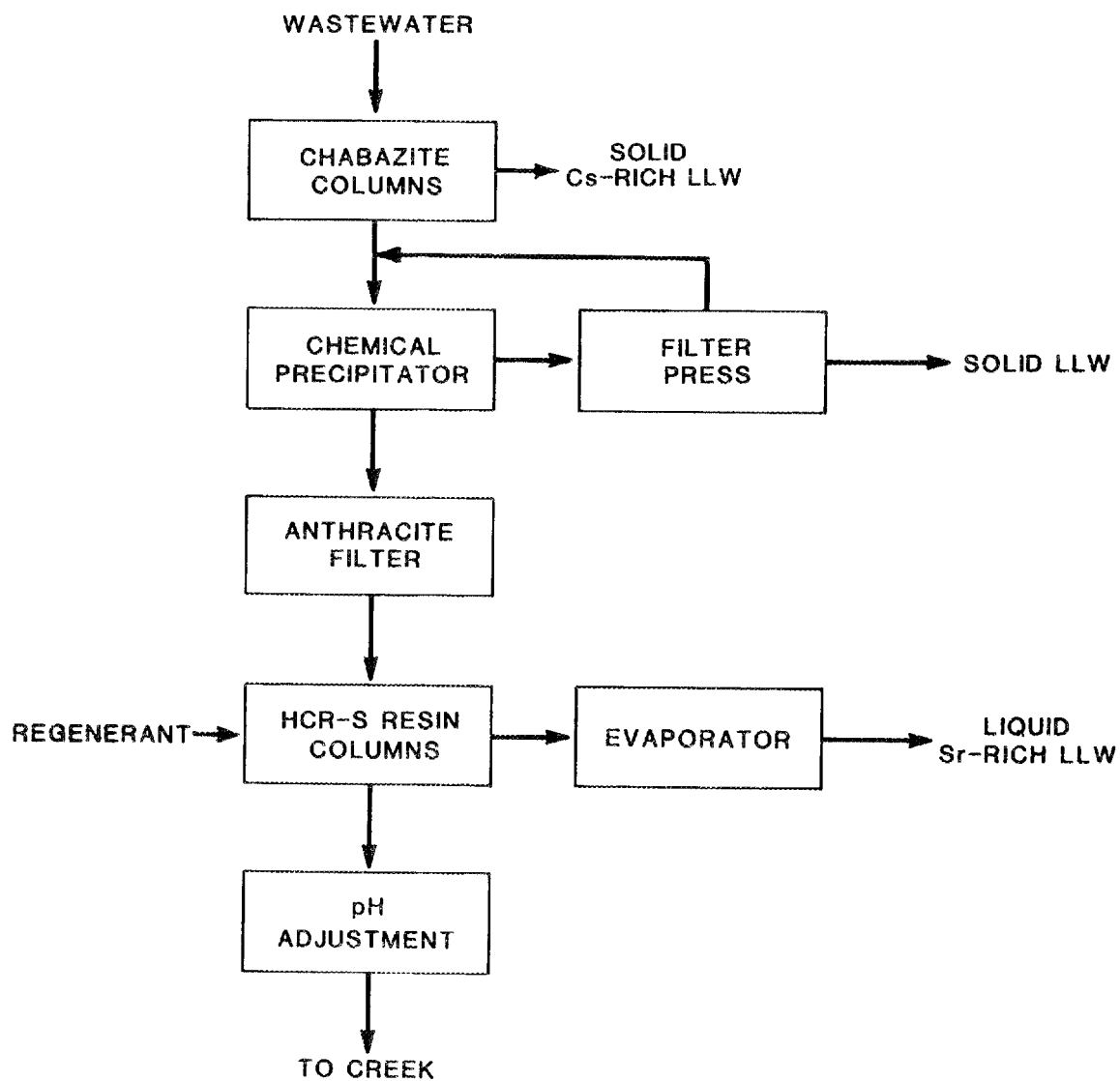


Fig. 1. Decontamination flowsheet for the Process Waste Treatment Plant.

ORNL DWG 86-1032

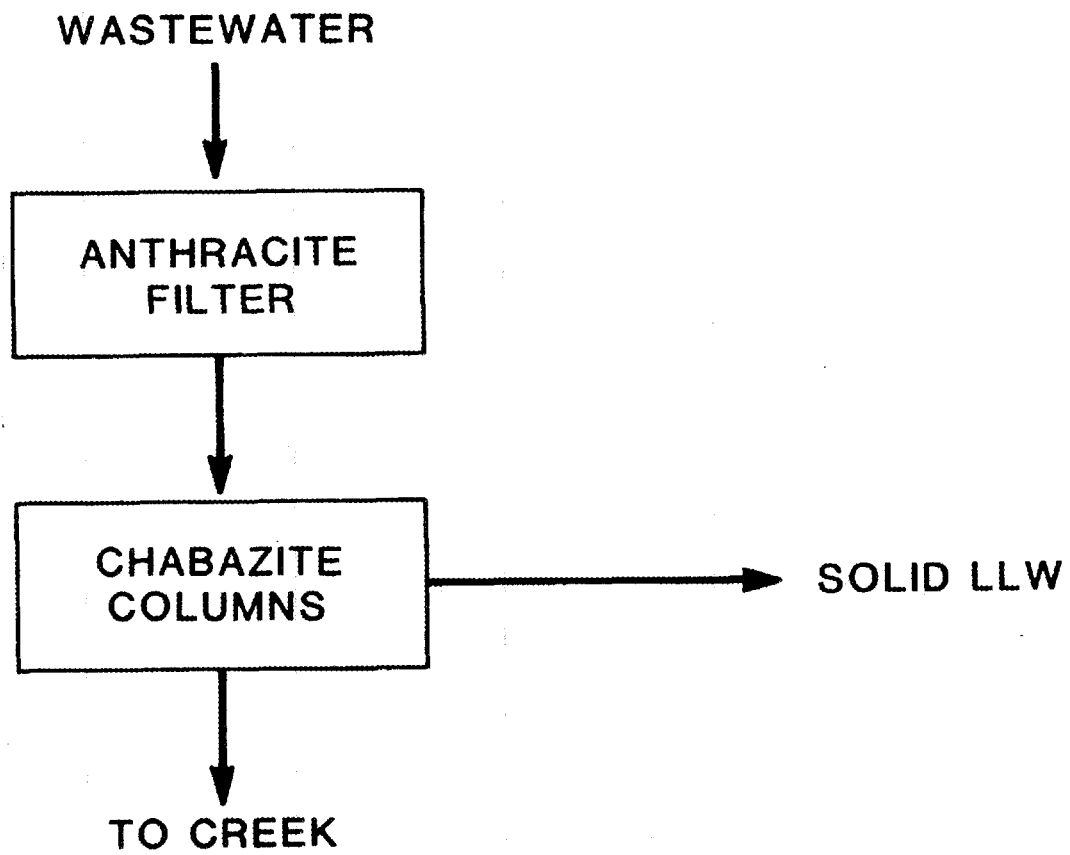


Fig. 2. Proposed decontamination flowsheet for the Process Waste Treatment Plant.

## 2. BACKGROUND

In December 1985 and January 1986, a significant spike occurred in the concentrations of  $^{90}\text{Sr}$  and  $^{137}\text{Cs}$  entering the PWT. This spike was caused by runoff through a construction site. Additional treatment equipment was needed temporarily to supplement the normal treatment plant. Thus, a decision was made to install skid-mounted equipment, leased on an emergency basis from the Chem Nuclear Company, and to perform a near-full-scale test of the improved chabazite treatment process using Ionsiv IE-95, a synthetic zeolite produced by Union Carbide, as the sorbent. Two  $3.7\text{-m}^3$  pressure vessel demineralizers (1.92 m in diam by 1.22 m in height) were used as ion-exchange columns for this test (see Fig. 3).

The columns were operated in series to treat process wastewaters with the following concentrations:

<u>Radionuclide</u>	<u>Range (Bq/L)</u>	<u>Average (Bq/L)</u>
$^{90}\text{Sr}$	2400-7100	4300
$^{137}\text{Cs}$	318-720	500

A total of  $6700\text{ m}^3$  (1810 BVs) of process wastewater was treated at a flow rate that gave an average residence time of ~13 min in each column. At the end of the test, the first column was approximately 50% saturated for  $^{90}\text{Sr}$ , and the  $^{90}\text{Sr}$  effluent concentration from the second column reached 310 Bq/L (see Fig. 4). No  $^{137}\text{Cs}$  breakthrough was detected at this point.

The distribution coefficient,  $K_d$  (shown in Fig. 4), is approximately equal to the number of BVs that have been processed at

ORNL DWG 88-594

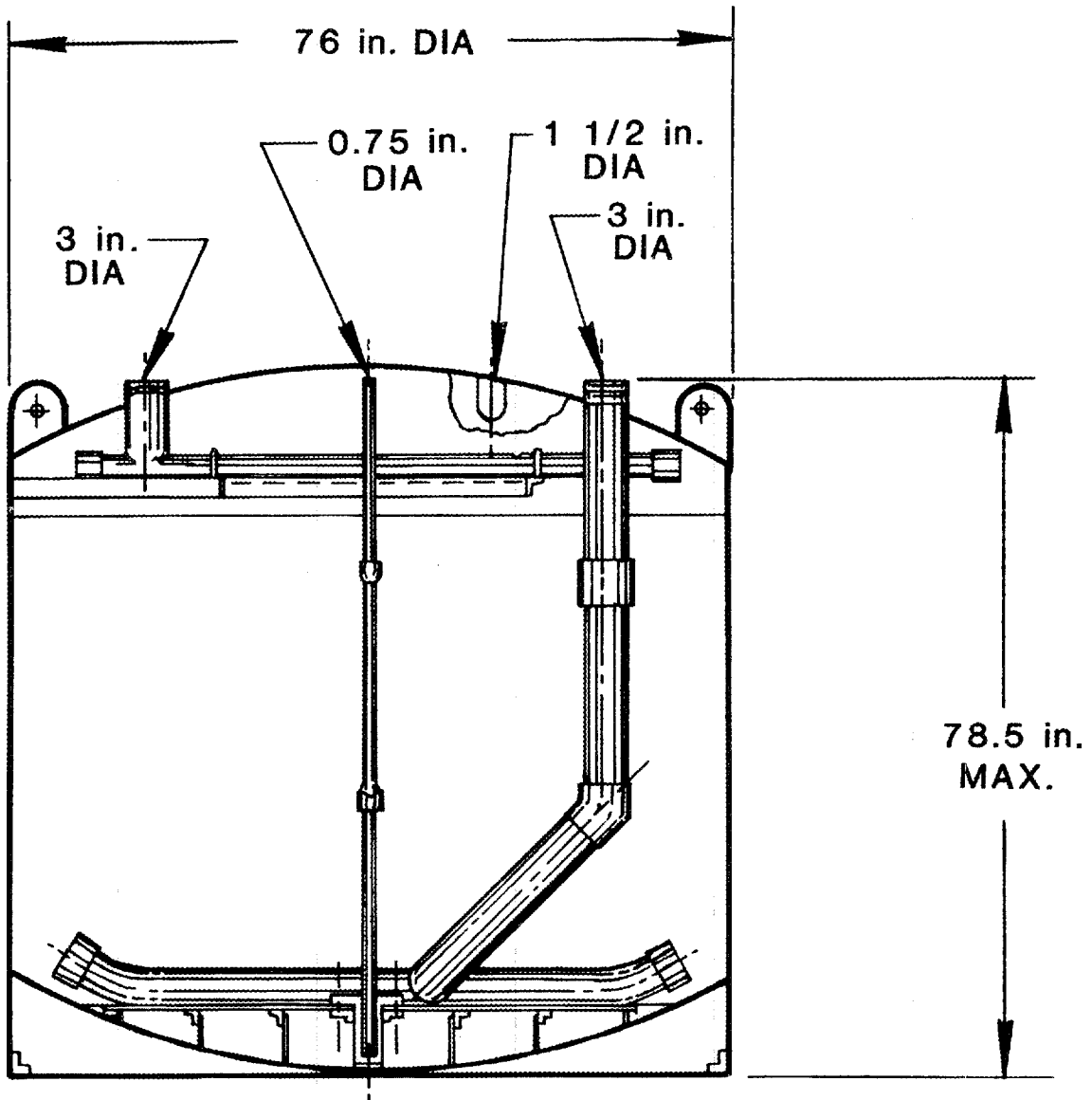


Fig. 3. Schematic of 3.7-m<sup>3</sup> pressure vessel demineralizers used in near-full-scale Ionsiv IE-95 zeolite tests.

ORNL DWG 86-11519R

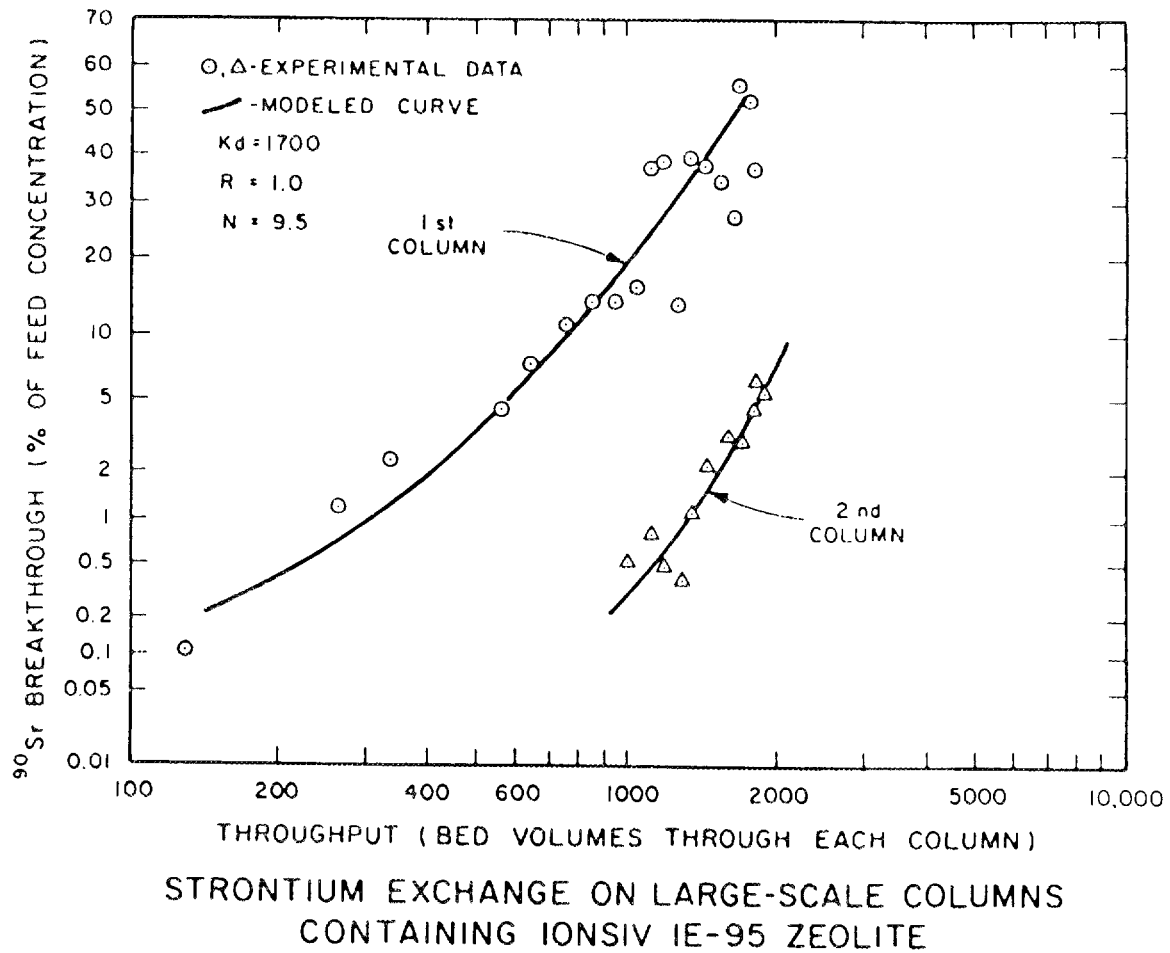


Fig. 4. Breakthrough data for near-full-scale test with Ionsiv IE-95 for  $^{90}\text{Sr}$  removal from process wastewater.

50% breakthrough. This factor is independent of the column operating conditions if equilibrium is met and should remain essentially constant for a given feed and sorption material. Therefore, it is often used to access the sorption capacity of a material for a specific application. The R and N are parameters of the Thomas model, which will be discussed later in Sect. 4.

These data indicated that the chabazite process had the potential to be a very simple, economical method for treating ORNL's process wastewater. However, the kinetics of the ion exchange were relatively slow. In order to effectively utilize the sorbent, four columns would need to be operated in series.<sup>1</sup> When the first column became loaded with  $^{90}\text{Sr}$ , it would be discarded, the second, third, and fourth columns would be moved forward one position (countercurrent to the flow of wastewater), and a new column would be installed at the fourth position.

A series of four smaller columns containing TSM-300 was used to test this flowsheet at 10% plant scale from April through June 1986. The configuration of the 0.57-m<sup>3</sup> pressure vessel demineralizers (0.76 m in diam by 1.22 m in height) used in this test are shown in Fig. 5. During the initial period of operation, algae growth in the equalization basin, which feeds the PWTP, was extremely high. Therefore, the first of the 3.7-m<sup>3</sup> columns (containing IE-95 loaded to >50% capacity for  $^{90}\text{Sr}$ ) was placed upstream of the TSM-300 columns to act as a filter. However, the IE-95 column still had a significant capacity to sorb cesium and a small capacity to sorb additional strontium. The concentrations of radionuclides in the IE-95 column feed and effluent are displayed below.

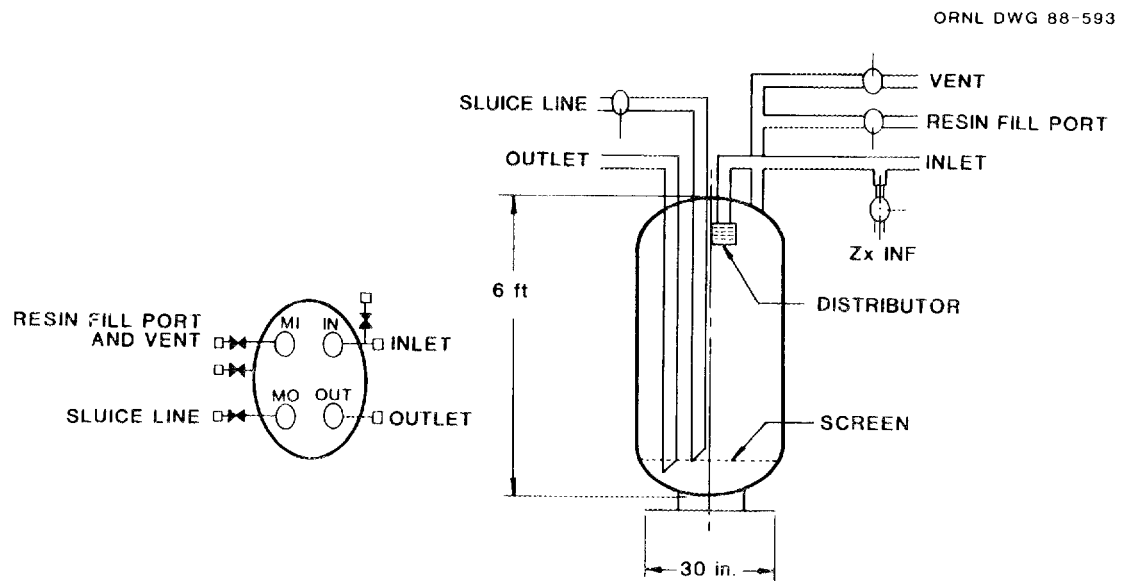


Fig. 5. Schematic of 0.57-m<sup>3</sup> pressure vessel demineralizers used in pilot-scale TSM-300 zeolite tests.

<u>Radionuclide</u>	<u>Feed range (Bq/L)</u>	<u>IE-95 column effluent range (Bq/L)</u>
Gross beta activity	3100-3700	780-2700
<sup>90</sup> Sr	1200-2900	690-2100
<sup>137</sup> Cs	380-460	<10

The feed to the series of TSM-300 columns was the effluent from the IE-95 column. The nominal flow rate through the four units in series was 3.4 m<sup>3</sup>/h (15 gal/min), giving the wastewater a residence time of 10 min in each column. The first zeolite column reached the 50% saturation for <sup>90</sup>Sr after ~6500 BVs had been processed (see Fig. 6). At this point, the second unit was at ~5% breakthrough, and the third and fourth units were both at <1% breakthrough. The distribution coefficient of 6500 for the TSM-300 was significantly higher than that of 1700 for the Ionsiv IE-95. The columns were shut down after processing 8200 BVs of wastewater because the first two units were partially plugged (presumably due to algae).

The data from the pilot-scale tests were modeled to predict full-scale operation by the method used to design zeolite columns at Three Mile Island.<sup>9</sup> The results indicated that the chabazite flowsheet, using TSM-300 as the sorbent, has the potential to reduce the total waste generation at the PWTP to 40% of its present level, and the long-term operating costs would also be ~40% of that for the existing plant.<sup>2,5</sup> Therefore, the zeolite in the first column of the series was replaced, and the system was put in a shutdown mode until testing could be continued.

The 3.7-m<sup>3</sup> columns containing Ionsiv IE-95 had processed 3075 and 1810 BVs of wastewater, respectively. Neither column had a large

ORNL DWG 87-1054

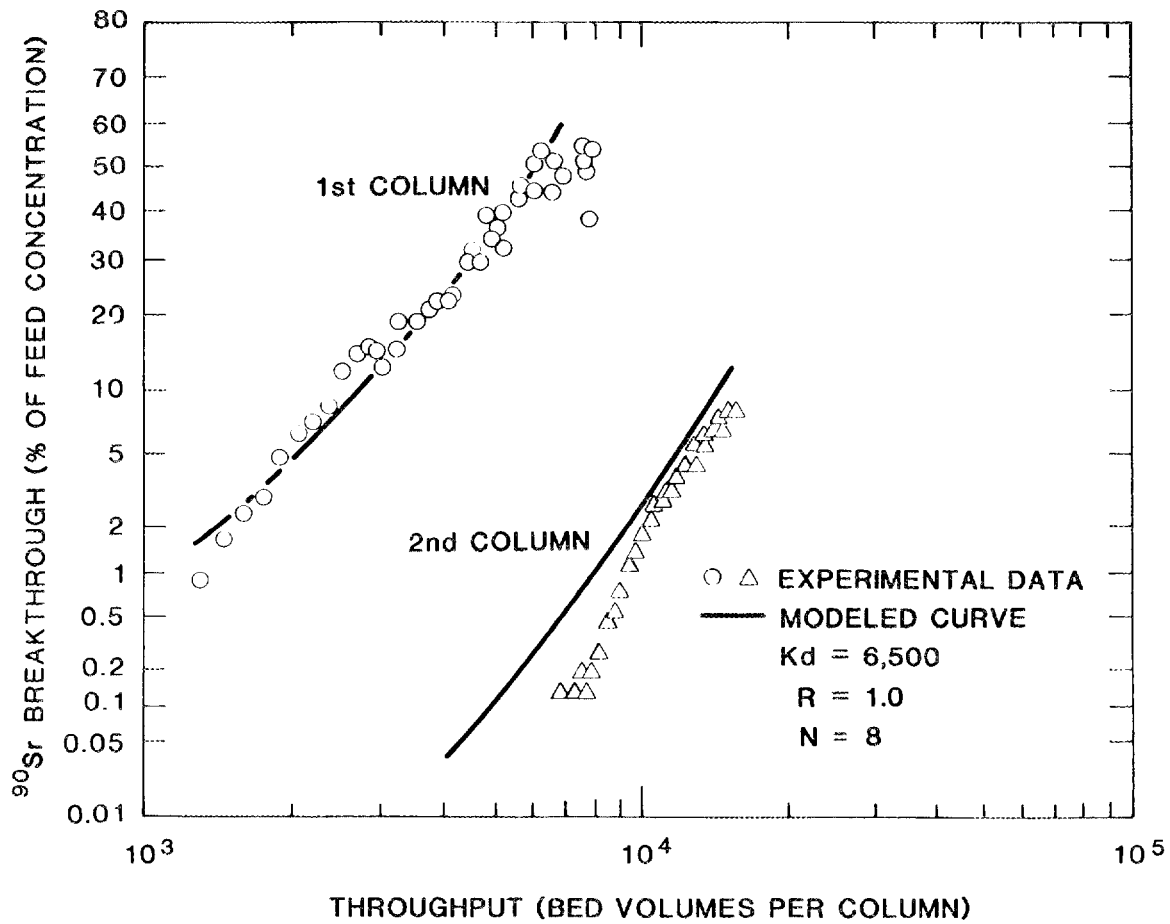


Fig. 6. Breakthrough data for pilot-scale test with TSM-300 zeolite for  $^{90}\text{Sr}$  removal from process wastewater with zeolite prefilter.

capacity for additional strontium removal, but both still had a significant capacity to sorb cesium. Therefore, the columns were stored until they could be installed at the head end of the PWTP and used to remove cesium from the PWTP feed.

### 3. EXPERIMENTAL RESULTS

Laboratory-scale test results<sup>4</sup> indicated that chabazites are capable of removing both  $^{137}\text{Cs}$  and  $^{90}\text{Sr}$  from ORNL's process wastewater. However, they have a much higher sorption capacity for cesium than strontium. Therefore, the studies in this report were focused in two areas: (1)  $^{137}\text{Cs}$  decontamination and (2)  $^{90}\text{Sr}$  and  $^{137}\text{Cs}$  removal. If chabazite columns were used only to treat cesium, they would need to be operated in conjunction with a strontium-removal process for use of the PWTP. In the second case, both Cs and Sr could be removed in a series of zeolite columns. Both concepts were tested in this study using the six zeolite columns described in the previous section. After the tests described in the previous section were completed, the six zeolite columns were backwashed and stored (filled with process water) for several months. They were then used for the two studies described in this report.

#### 3.1 NEAR-FULL-SCALE COLUMNS FOR $^{137}\text{Cs}$ DECONTAMINATION

Each 3.7-m<sup>3</sup> ion-exchange column containing Ionsiv IE-95 was used in the PWTP to remove cesium from the wastewater using the configuration shown previously in Fig. 1. The object of this test was to verify modeling results obtained from laboratory-scale tests and to determine if factors other than the sorption capacity of the zeolite would determine the life of the column; i.e., column plugging.

A sand filter (containing 0.3 to 0.84 mm of sand) and the 3.7-m<sup>3</sup> Ionsiv IE-95 columns (one at a time) were installed at the head end of the PWTP. The maximum flow rate obtainable through the sand

filter was 23 m<sup>3</sup>/h (100 gal/min). Since the PWTP often operates at 34 m<sup>3</sup>/h (150 gal/min), the feed was split with 17 m<sup>3</sup>/h (75 gal/min) (or less depending on the pressure drop across the two units) passing through the filter and zeolite column. This waste stream then joined the remaining feed before going through the remaining process steps. This system was operated continuously from February through November 1987. The results are summarized in Table A.1 in the appendix.

The column that was used as the first column in the emergency campaign and as the prefilter for the pilot-scale units broke through with <sup>137</sup>Cs immediately when put on-line on September 13, 1987. Laboratory-scale tests of a sample from the top of the column (which should have the lowest remaining sorption capacity for cesium) indicated that the column had not lost any of its sorption capacity. This led to the conclusion that the bed was plugged with algae and solids from the equalization basin and that channeling was occurring within the column. This is not surprising since the column was used without a prefilter for ~3000 BVs in previous tests. Backwashing could not rejuvenate the column and it was removed from service.

The second column from the emergency campaign had been partially spent for <sup>90</sup>Sr, but had not seen <sup>137</sup>Cs during the previous test. This column was operated at the PWTP from February 2, 1987, to December 3, 1987, to process 22,700 BVs (22,500,000 gal) of wastewater. During this time, the <sup>137</sup>Cs concentration in the feed ranged between 100 and 320 Bq/L, with an average of 160 Bq/L. The effluent concentrations are shown in Fig. 7. Cesium breakthrough began to occur between 4000 and 8000 BVs. The effluent values varied between 8 and 25% breakthrough

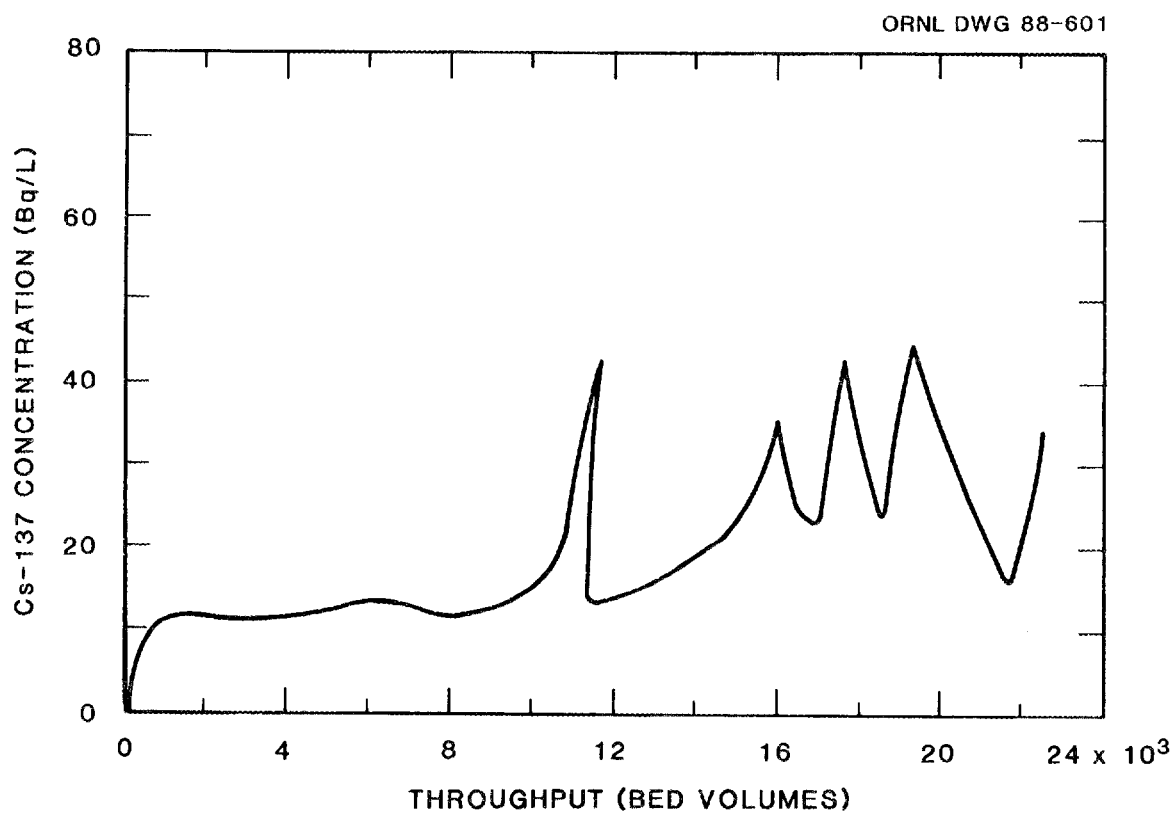


Fig. 7. <sup>137</sup>Cs effluent concentration from near-full-scale Ionsiv IE-95 columns for treatment of process wastewater.

during the remainder of the test (except one value that reached 54% and is probably an analytical error). The effluent concentrations were usually <30 Bq/L, and 45 Bq/L was the maximum effluent concentration obtained over the 10-month period. The effluent concentration was still well below the proposed limit of 111 Bq/L when the run was terminated because of column plugging. If the breakthrough curve is extended, the distribution coefficient can be estimated to be 63,000 (which is extremely high).

The column was initially operated at 17 m<sup>3</sup>/h (75 gal/min) to yield a residence time of ~13 min. However, the pressure drop across the column would increase until the flow rate was significantly reduced (as indicated by high-residence times in Fig. 8). This increase could be due to the buildup of solids that passed through the coarse sand filter, to chemical reactions between the feed and the zeolite, or to degradation of the zeolite. The zeolite bed initially required backwashing to reduce the pressure drop after ~8000 BVs and approximately every 4000 BVs thereafter. After 22,000 BVs were processed, the pressure drop could no longer be reduced by air sparging and backwashing, and the system was therefore shut down.

It should be noted that air sparging and backwashing were adequate to return the system to its original capacity over several cycles. However, near the end of the test the pressure buildup across the column increased very quickly after backwashing. This indicates that backwashing was not complete during this period, and total plugging occurred quickly thereafter. This is significant because the column used in this experiment was not designed for backwashing. With a

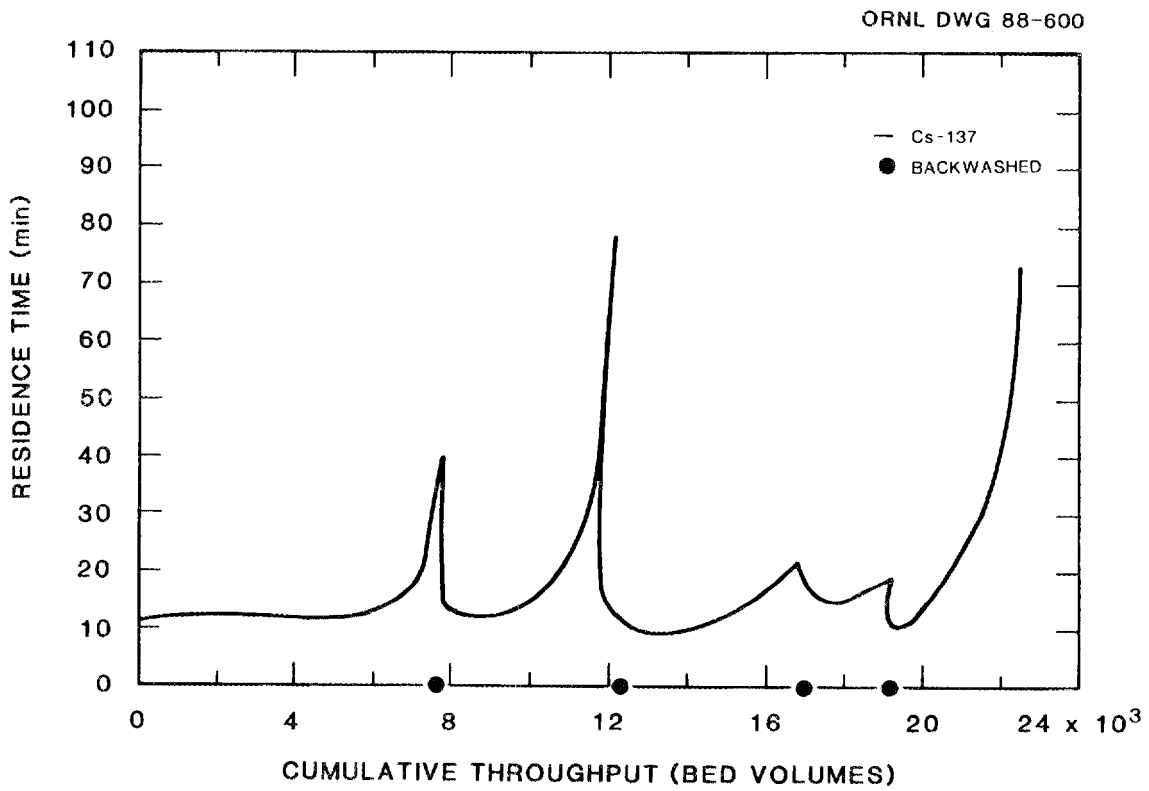


Fig. 8. Residence times for near-full-scale columns containing Ionsiv IE-95 zeolite.

properly designed unit, the life of the column could have possibly been extended.

This test successfully demonstrated the feasibility of using chabazites to remove  $^{137}\text{Cs}$  from ORNL process water. The procedure is simple and reliable and only requires occasional backwashing (once every 1-2 months for this system). The backwashing operation was very cumbersome for this experimental unit; however, proper design of permanent equipment could overcome the problems encountered during this test.

### 3.2 PILOT-SCALE COLUMNS FOR $^{90}\text{Sr}$ AND $^{137}\text{Cs}$ DECONTAMINATION

The four  $0.57\text{-m}^3$  columns containing TSM-300 were used to treat ORNL process wastewater for both  $^{137}\text{Cs}$  and  $^{90}\text{Sr}$ . They were operated from April to November 1987 (parallel to the existing PWTP system) to (1) demonstrate the feasibility and develop operating techniques for operating four columns in series, (2) verify the laboratory-scale modeling results, and (3) determine parameters that would be important in the design of full-scale equipment.

This system was initially operated in the summer of 1986 and shut down for ~9 months prior to this test. This original test had been terminated because of high pressure drops in the first two columns. Prior to shutdown in 1986, the first column was refilled with fresh zeolite and filled with process water. The zeolite in the second column was also replaced prior to the beginning of this study in order to start with material which was essentially uncontaminated with  $^{90}\text{Sr}$  and  $^{137}\text{Cs}$ . These reloaded columns were placed at the end of the train.

At the beginning of this test, the first column in the train (third in the 1986 test) had processed 1500 BVs of wastewater containing 50 to 130 Bq/L  $^{90}\text{Sr}$  and no  $^{137}\text{Cs}$ . The second column had only processed uncontaminated wastewater.

A portion of the feed for the Ionsiv IE-95 column (down stream of the roughing sand filter described in Section 3.1) was routed to the four  $0.57\text{-m}^3$  columns for this test. The flow rate was set at  $0.057\text{ m}^3/\text{min}$  (15 gal/min) to maintain the 10-min residence time per column required to overcome the slow kinetics of the chabazite material.<sup>1</sup> The feed concentration during this period ranged between 700 and 1400 Bq/L  $^{90}\text{Sr}$  and 100 to 300 Bq/L  $^{137}\text{Cs}$ . The operational data are listed in Tables A.2 and A.3 in the appendix and summarized in the following text.

The system was operated by replacing the first column in the series when it became loaded with strontium. When the first column reached ~50% breakthrough, it was taken off-line. The spent zeolite was hydraulically transferred to a high-integrity container for permanent disposal. The column was refilled with fresh zeolite (hydraulically transferred with a double-diaphragm pump), backwashed to remove fines, and moved to the end of the train. Therefore the second, third, and fourth columns were moved forward one position (counter-current to the flow of wastewater) each time a column was replaced. This sequence completed one cycle.

The system was operated for six cycles over a 7-month period. Four of these cycles were operated for an average of 3400 BVs (510,000 gal) until the first column had reached 60 to 80% breakthrough

for  $^{90}\text{Sr}$ . The two remaining cycles were for only 600 and 750 BVs. One of these cycles was cut short because the two previous columns were run well past the 50% breakthrough point. Modeling results<sup>5</sup> have indicated that the first column must be removed at approximately the 50% breakthrough point to obtain a steady operating system. Otherwise, a column will have to be pulled prematurely to meet discharge limits. The other column, which was inactive for 9 months, had shown operational problems at every position in the train. None of the other columns indicated that the 9-month shutdown had caused negative effects.

The  $^{90}\text{Sr}$  breakthrough curves for the first column of the four longer cycles are shown in Fig. 9. They are all similar, except that the second cycle had a slightly higher initial breakthrough. No  $^{137}\text{Cs}$  was detected in the effluent of any of the columns. The distribution coefficient was only 3100 for these cycles, compared to 6500 for the 1986 test when the feed contained no cesium but higher strontium concentrations.

The  $^{90}\text{Sr}$  effluent concentrations from the system (from the fourth column in the series) ranged between 1 and 30 Bq/L, as shown in Fig. 10. During all but one cycle, the effluent concentration started at ~30 Bq/L (which was higher than the feed concentration for that column), dropped to a minimum of ~6 Bq/L, and then increased. These columns were designed such that ~5 cm of zeolite remain in the bottom of each column below the sluice line (see Fig. 5) when the loaded zeolite is removed. Therefore, loaded zeolite was always present in the bottom of the last column in the series. When decontaminated water

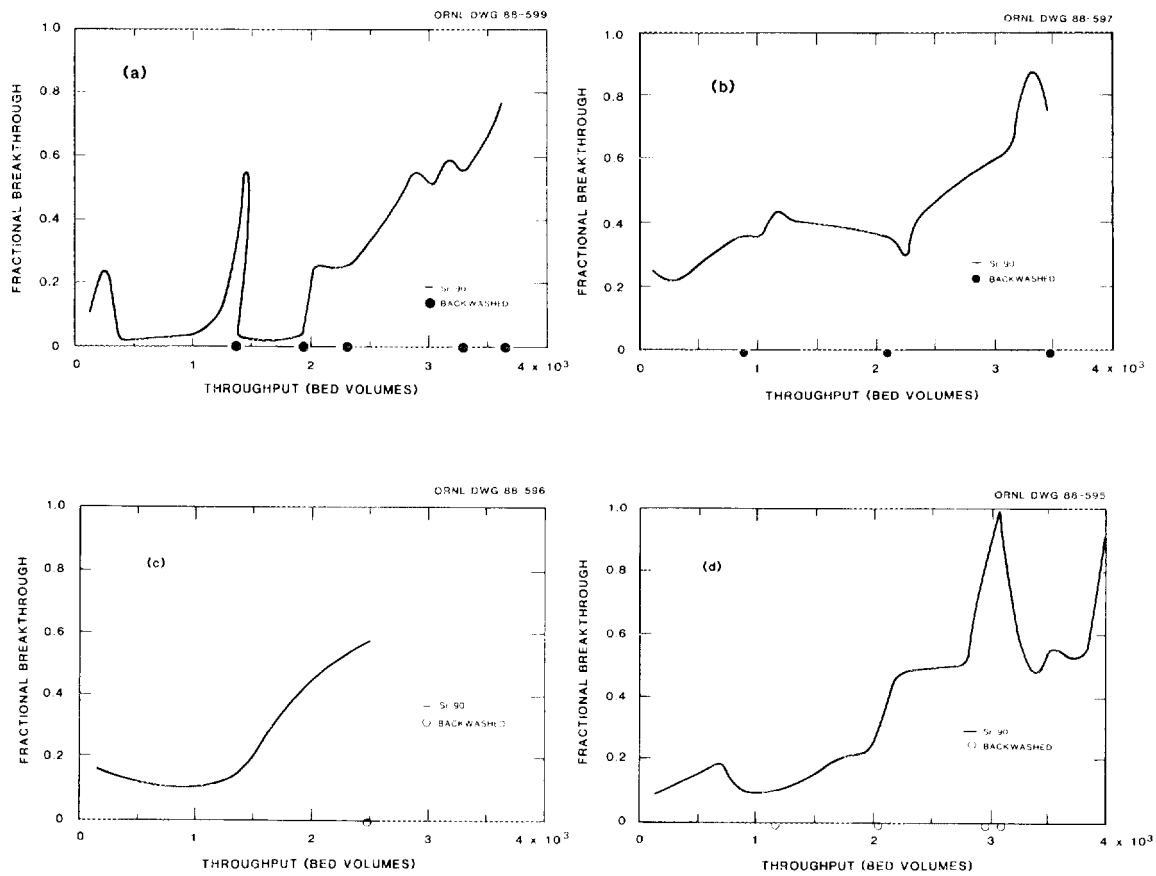


Fig. 9. Breakthrough data for first column in pilot-scale test with TSM-300 zeolite for  $^{90}\text{Sr}$  removal from process wastewater. A = first cycle, B = second cycle, C = third cycle, and D = fourth cycle.

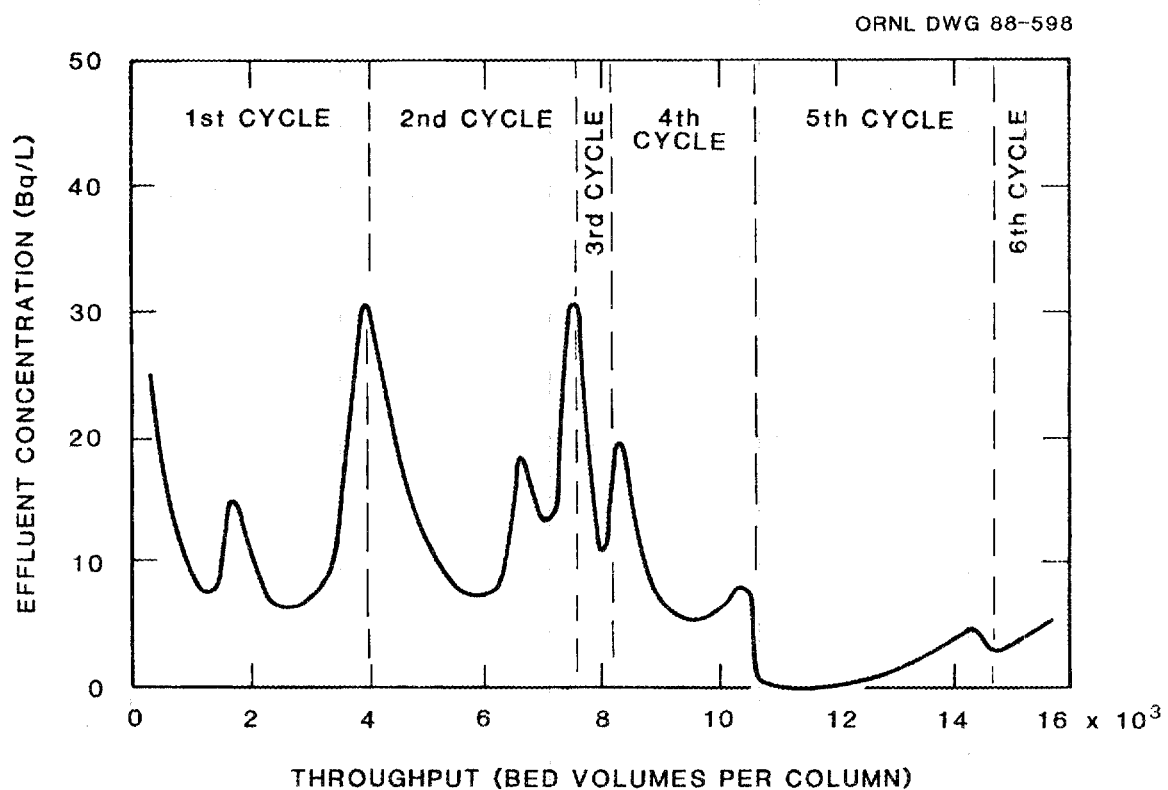


Fig. 10.  $^{90}\text{Sr}$  effluent concentrations from TSM-300 pilot-scale test for treatment of process wastewater.

first contacted this loaded material,  $^{90}\text{Sr}$  was leached off the zeolite. This caused an initial increase in the strontium concentration at the beginning of each cycle. After this initial increase, a typical breakthrough wave developed.

The effluent data for the fifth cycle are more typical of ion-exchange data. Extreme effort (tilting, banging sides of the column, etc.,) was taken to remove most of the loaded zeolite from the fourth column for this run. During this cycle, the concentration remained below 2 Bq/L for 2500 BVs, and the maximum  $^{90}\text{Sr}$  concentration was 7 Bq/L. These data are an indication of the minimum effluent concentration that can be expected from properly designed columns.

The system effluent data verified two important points about the chabazite system. The data indicate that the design of the columns will be a major factor in determining the effluent concentration and waste generation rates in a full-scale system. The data also indicate that  $^{90}\text{Sr}$  will be leached off loaded zeolites if they come in contact with water during storage or disposal. Posttreatment will be required to reduce leachability of the zeolites, or they will have to be stored in high-integrity containers.

Several other operational problems were encountered during this experiment. Pressure buildup across these columns occurred much quicker than with the Ionsiv IE-95 columns. For example, the columns required backwashing every 500 to 1000 BVs. This was initially contributed to fines that had passed through the sand filter (construction work had caused the feed to contain a large amount of silt during the early part of the summer) and to algal growth from the

equalization basin. However, during the latter part of the summer, the biogrowth problems in the equalization basin were controlled by regular spraying with Cutrine, a copper-based solution. It was noted during this stage of operation that copper was being removed in the columns (from 0.2 to 0.8 ppm to as low as 0.03 ppm) by adsorption onto the zeolite or by killing algae inside the column.

The following backwash procedure was necessary to eliminate pressure buildup in this experimental system. The column was air-sparged for 15 min and backwashed with process water until the effluent was clear of algae and fines. A significant fraction of the pressure drop across the first column was due to plugging in the inlet distributor (a Johnson screen), and it was necessary to backwash the inlet distributor to the first column. This indicates that the sand filter was not adequately removing fines from the feedwater. The full-scale system will require better prefilter equipment. Finally, the column was washed with process water in the normal down-flow mode before use in the system. A large amount of fines was removed during this step, indicating that these demineralizers are not properly designed to achieve adequate backwashing of zeolite beds.

The zeolite particles were usually "cemented" together after processing 3000 to 4000 BVs and had to be broken apart with a high-pressure water lance before they could be backwashed or removed from the column. During the portion of the summer when Cutrine was used regularly, the zeolites were clumped together by an amorphous, gelatinous material. This transparent matrix contained zeolite fines and other detritus, little algae, and no identifiable bacteria.

The  $^{90}\text{Sr}$  effluent concentration often decreased slightly after backwashing and then tended to return to its original value rather rapidly. This can probably be attributed to the fact that backwashing opens the cemented areas of the bed and allows the wastewater to contact more of the zeolite surfaces. The gelatinous material surrounding the particles must certainly lower the mass transfer between the water and the zeolite, which may account for the lower distribution coefficient obtained during this test. The life of the columns could probably be extended significantly if plugging was eliminated.

During the 7-month period of operation, 15,000 BVs (2,250,000 gal) of wastewater was treated and 6 BVs (900 gal) of spent zeolite were produced. This exercise successfully demonstrated the feasibility of using chabazite columns operated in series to remove both  $^{90}\text{Sr}$  and  $^{137}\text{Cs}$  from ORNL process wastewater. However, two areas were identified that need further investigation before a permanent system is installed at the PWTP. Plugging of the columns is limiting the life of the chabazites, and posttreatment is needed to reduce the hazard of storing or disposing of the secondary solid waste.

Plugging was much worse in the pilot-scale columns. If plugging is a result of zeolite degradation or chemical reaction with the feed, the following two major differences between the two systems may be contributing factors: (1) the columns contain different zeolites and (2) the flux across the columns is different. The natural material (TSM-300) may physically degrade easier than Ionsiv IE-95, which contains a synthetic binder. The differences in chemical composition

could result in different reactions with the feedwater. The flux across the pilot-scale units is also higher. Physical degradation of the particles could be worse at the higher flux. However, both materials were tested at high flux rates for up to 20,000 BVs on a laboratory scale, and no plugging problems were seen. Additional tests will be needed to determine the causes of plugging.

#### 4. MODELING OF EXPERIMENTAL RESULTS

One of the most critical aspects of the scaleup of adsorption and ion-exchange systems involves characterization of the effluent concentration profile as a function of throughput. This profile, commonly referred to as the breakthrough curve, represents the specific combination of equilibrium and rate factors that control process performance in a particular application.

However, very little has been done in the way of predictive modeling of fixed-bed multicomponent liquid systems, and a general analytical solution to fixed-bed ion exchange developed by Thomas is commonly used for the basis for design of ion-exchange columns.<sup>10</sup> Thomas assumed that ion-exchange mass transfer could be approximated by a second-order kinetic equation and modeled by the following three parameters: (1)  $T$ , a throughput parameter; (2)  $N$ , column height as transfer units; and (3)  $R$ , the separation factor. For dilute solutions, such as those used in this study,  $R$  and  $T$  are unity. The value of  $N$  is determined from experimental breakthrough curves and used to predict scaleup. (See Appendix B for details.)

The Thomas equation models the loading of one ion-exchange column. The model has been extended by R. M. Wallace to predict operation of several columns in series. He uses a numerical analysis solution of the Thomas equation with input values of  $R$ ,  $N$ , and  $K_d$ .<sup>9</sup>

Breakthrough curves were obtained for the near-full-scale and pilot-scale data taken in this study by plotting the mean throughput, measured in BVs, vs the normalized Sr concentration (effluent/mean feed

concentration) on log-normal probability paper. The resulting curves are shown in Figs. 11 and 12.

These were compared with previous pilot- and laboratory-scale ion-exchange test data.<sup>1,3,4</sup> Here lab-scale experiments were performed in 1.27-cm-OD columns which contained 6.5 to 20 mL of Ionsiv IE-95 and two samples of TSM-300. The columns had 2.3 to 7.1 length-to-diameter ratios and 1 to 7 min residence times. The resulting modeling parameter values are summarized in the first five columns of Table 2.

The models predict the experimental data reasonably well. The models are less accurate for the initial portion of the breakthrough curve where analytical techniques make the experimental data questionable for extremely low values of  $^{90}\text{Sr}$ . All breakthrough curves for each zeolite had the same value of  $K_d$ , regardless of feed composition, flow rate, residence time, and column configuration, except the prefiltered pilot-scale data taken in 1986. This result indicates that the assumption of a trace system is valid.

The curves for the laboratory-scale columns show the expected trends with  $N$  and the slope of the breakthrough curve increasing with residence time and/or column length. However, the values of  $N$  decrease for the pilot-scale columns. The same trends were seen for  $^{137}\text{Cs}$  data (i.e.,  $N$  decreased significantly with scaleup).

Next, the laboratory-scale column was used to predict scaleup. Values for  $N$  were predicted from the laboratory-scale data by taking the ratio of Eq. (6)\* with each set of operating conditions, as

---

\*All equations are listed in Appendix B.

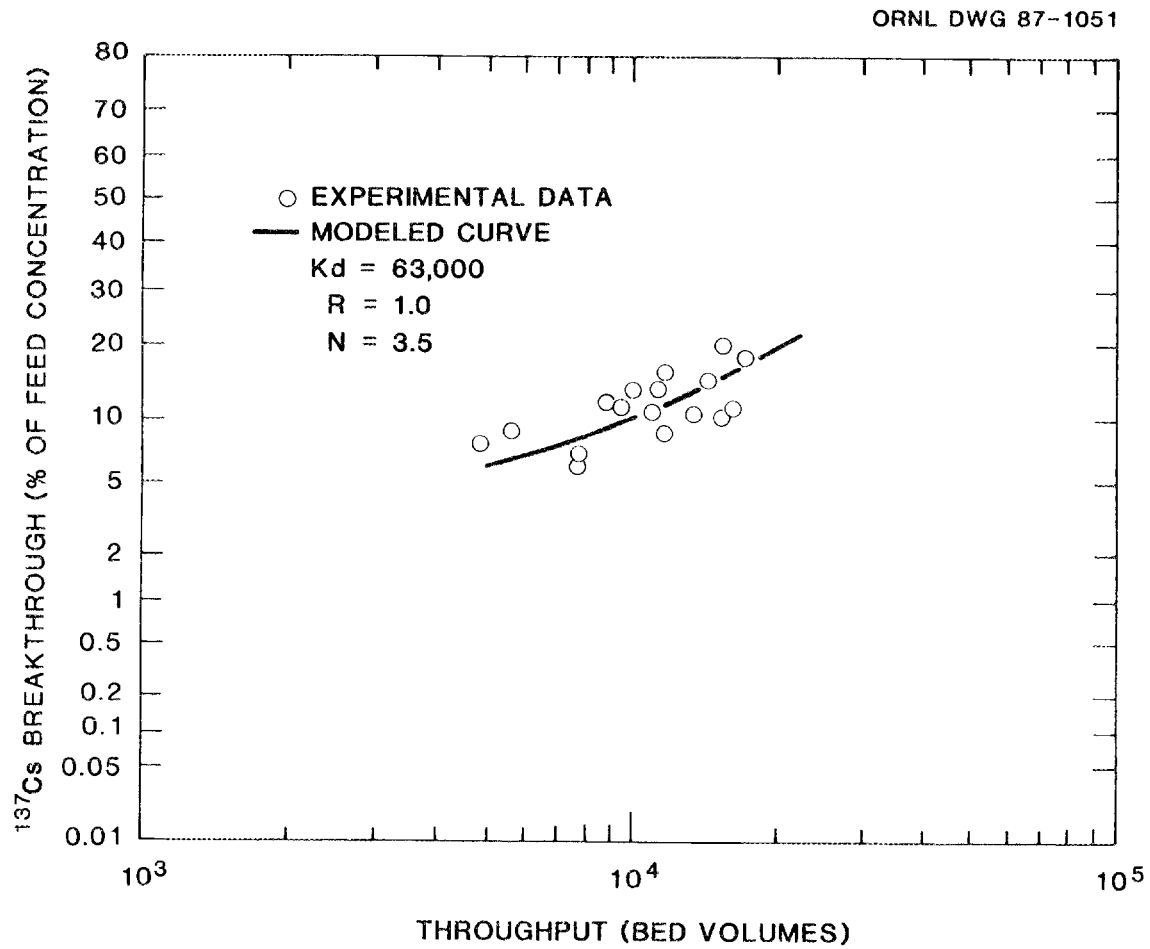


Fig. 11. Modeled breakthrough curve for near-full-scale test with Ionsiv IE-95 for  $^{137}\text{Cs}$  removal from process wastewater.

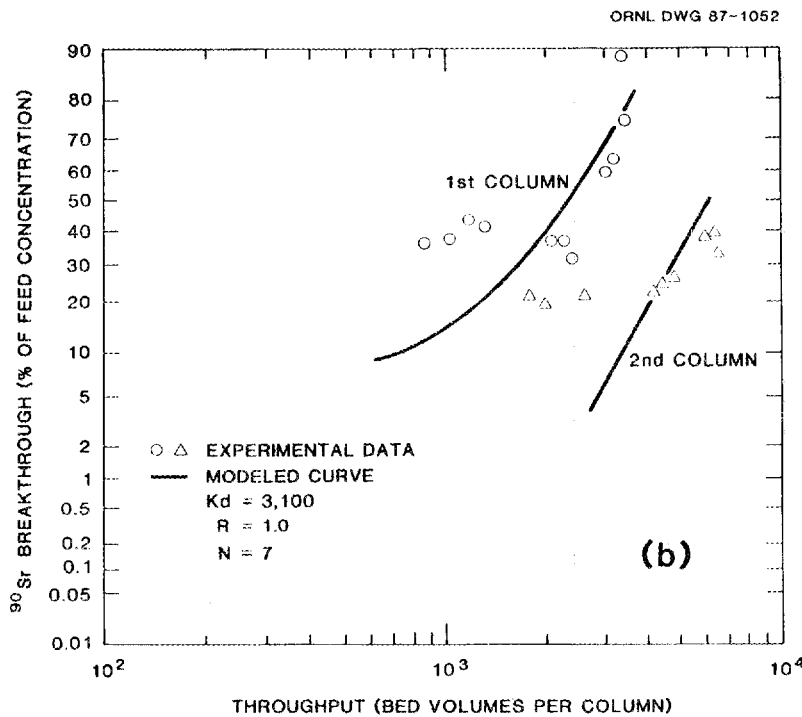
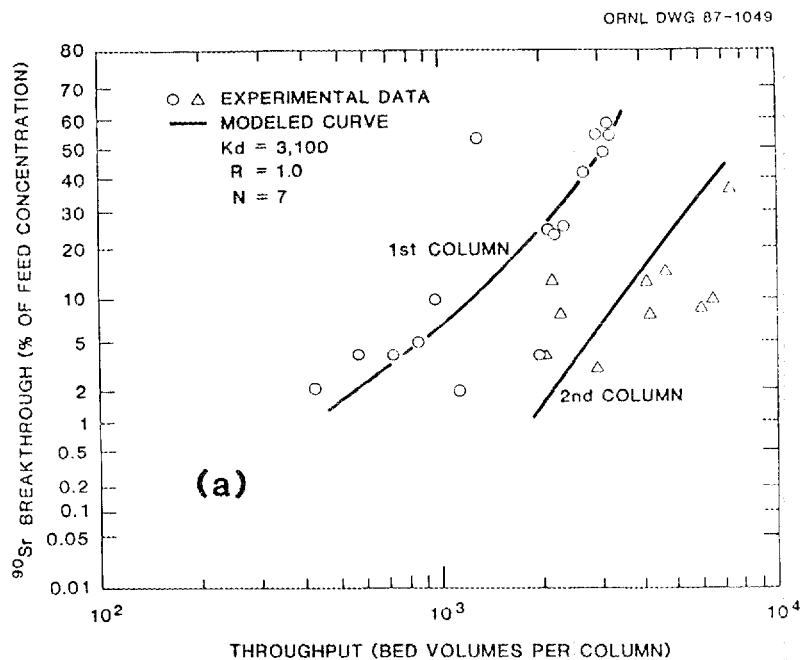


Fig. 12. Modeled breakthrough curve for pilot-scale test with TSM-300 zeolite for  $^{90}\text{Sr}$  removal from process wastewater. (A) first cycle and (B) second cycle.

Table 2. Predicted values of N for scaleup of  $^{90}\text{Sr}$  laboratory data

Zeolite type	Column diameter (cm)	Zeolite volume (mL)	Direct modeling of data		Controlling mass-transfer mechanism			
			$K_d$	N	Pore or particle	Fluid phase	Axial dispersion	Molecular diffusion
IE-95	1.53	6.5	2,350	5.0	--	--	--	--
IE-95	1.53	20	2,350	6.5	30	22	15	8
IE-95	1,930.00	376,000	2,350	6.0	57	99	170	530
TSM-300-AL	1.53	6.5	2,450	2.0	--	--	--	--
TSM-300-AL	1.53	20	2,450	3.8	5	8	6	4
TSM-300-D	1.53	20	3,100	16.7	--	--	--	--
TSM-300-D	76.20	566,000	3,100	7.0	24	68	19	150
TSM-300-D <sup>a</sup>	76.20	566,000	6,500	8.0	--	--	--	--

<sup>a</sup>With pretreatment.

traditionally done at ORNL.<sup>1,5,9</sup> This is equivalent to  $a = 0$  in Eq. (14). The experimental data indicate that  $K_d$  is constant for each ion-exchange material, and trace-system theory indicates that  $K_a$  is independent of the controlling mass-transfer mechanism. Therefore,  $K_a$  was assumed to be a constant during scaleup, and  $N$  was assumed to be a function of  $v/f$  only. Based on these assumptions,  $N$  should be directly proportional to the change in residence time. Calculated values of  $N$  are shown in the sixth column of Table 2. This scaleup equation predicts high values of  $N$ .

Equation (14) was used to predict scaleup for other controlling mass-transfer mechanisms. The results are shown in the last three columns of Table 2. For all values of  $a$ ,  $N$  tended to converge toward the experimental value when the volume in the laboratory-scale column was varied ( $S$  remained constant) but diverged for the pilot-scale data where  $S$  increased. All mechanisms predicted high values of  $N$ . The molecular diffusion mass-transfer mechanism comes closest to modeling the laboratory-scale data. However, it is most likely that film or pore diffusion, not molecular diffusion, is the controlling mechanism.

These results indicate that  $K_a$  changes during scaleup.  $N$  may be independent of the controlling mass-transfer mechanism when modeling a given breakthrough curve, but the controlling mechanism must be taken into account during scaleup. The results also indicate that combined or changing resistances may be controlling the mass-transfer rate.

There is a good chance that channeling was a contributing factor in the pilot-scale tests. Channeling, coupled with radial and axial dispersion in large-diameter columns, will cause the breakthrough curve

to be "broad," reducing the slope of the curve.<sup>11</sup> This phenomenon would tend to lower the effective value of  $N$  for the larger scale columns. However, laboratory-scale data (where plugging was not a problem) were not modeled very accurately.

Appropriate values of  $N$  (determined by direct fitting each experimental breakthrough curve with the Thomas equation) were used in Eq. (15) to determine if the change in slope of the breakthrough curve could be accurately predicted for changes in  $N$  during scaleup. The slopes for each curve were accurately predicted over the full range of  $X$  and  $T$  using  $B = 0.5$ .

This modeling exercise has shown that the Thomas equation can be used to accurately model trace multicomponent systems. However, accurate scaleup predictions cannot be made unless a single controlling mechanism is known to control mass transfer. The diffusivity must also be known in order to predict how the number of theoretical transfer units change with operating conditions. Once these values are known, the slope of the new breakthrough curve can be accurately predicted from laboratory-scale data. If combined mass-transfer resistance is the controlling mechanism, Eq. (14) cannot be used to predict scaleup.

## 5. ECONOMIC ANALYSES

The laboratory- and pilot-scale data taken prior to 1987 were modeled<sup>5</sup> to determine the waste generation rates that could be expected at plant scale and determine the most cost-effective processes to be considered for further development. The waste generation rates and equipment sizes were determined by using the Thomas and Wallace models. Future-value economic analyses<sup>12</sup> were then used to compare the relative long-term costs of potential flowsheets. Estimated capital and operating costs, including costs for the disposal of secondary waste streams, were used to determine future value costs for each flowsheet, assuming startup in 1989 with a 15-year plant life. The results from this study are summarized in Table 3. The study indicated that the chabazite flowsheet would produce the least amount of waste and would be the least expensive process to install and operate. These results were the basis for continued development of the chabazite flowsheet.

The analyses shown in Table 3 were based on a plant throughput of 9.45 L/s (150 gal/min), assuming the feed contains an average of 4000 Bq/L <sup>90</sup>Sr and 400 Bq/L <sup>137</sup>Cs. The flowsheets were evaluated assuming the maximum effluent concentrations would be 32 and 15 Bq/L, respectively. This produces a total fractional release that is less than one based on the proposed DOE limits (37 for <sup>90</sup>Sr and 111 Bq/L for <sup>137</sup>Cs). The flowsheets were developed for a train of four 3.7-m<sup>3</sup> columns in series for the TSM-300 flowsheet and the existing configuration for the HCR-S resin flowsheet. The waste generation calculations include the total solids and concentrated secondary

Table 3. Comparison of alternative flowsheets for PWTP upgrade<sup>a</sup>

Flowsheet name	Waste generation (m <sup>3</sup> /year)	Future value (\$M in 2004)
Chabazite	57	8.3
CSA <sup>b</sup>	16	11.5
Clinoptilolite	72	16.6
IRC-84	76	18.6
HCR-S	142	22.5
Chabazite <sup>c</sup>	120	13.5
HCR-S <sup>c</sup>	142	22.5

<sup>a</sup>Based on laboratory- and pilot-scale data taken in 1986 unless otherwise indicated.

<sup>b</sup>Manufacturer of continuous countercurrent ion-exchange columns.

<sup>c</sup>Based on pilot-scale data taken in this study.

wastes, but do not include volume increases that might occur as a result of postprocessing prior to permanent disposal.

Cost comparisons for the flowsheets were made by calculating the "future costs" of each plant based on a startup date of 1989 and a plant life of 15 years. The cost estimates were based on the assumption that the given flowsheet would be used to replace the existing PWTP facility. Most major equipment items were replaced with upgraded equipment, but it was assumed that the existing building would be used. If the existing plant was kept for a backup facility, additional space requirements might be necessary. No salvage value or decommissioning costs were taken into account. Costs for post-treatment of the waste generated at the PWTP were estimated in the disposal costs, but facility costs were excluded from this study. The inflation rate was assumed to be 4% in 1986, 3% in 1987, 4% in 1988, 5% in 1989, and 5.5% through 2004.<sup>13</sup>

It should be noted that these costs are based on order-of-magnitude estimates and should be used for comparison purposes only.

The major assumption that was made in these analyses is that there is a linear relationship between the residence time and N, the number of theoretical stages required to meet discharge limits. As the data in Sects. 4 and 5 indicated, this may not be a valid assumption. Data to date indicate that N will remain essentially constant for a given scale, regardless of operating conditions.

Therefore, the chabazite and HCR-S flowsheets were reevaluated using the data generated in this study. The results are also summarized in Table 3. Neither the waste generation rate nor the long-

term costs were significantly different for the existing flowsheet. The costs and waste generation rate were increased for the chabazite flowsheet. Nevertheless, the waste generation and total operating costs for the lifetime of the plant is lower than that for the HCR-S flowsheet. The remaining flowsheets will have to be tested at the larger scale in order to determine their waste generations and costs relative to the chabazite flowsheet.

## 6. CONCLUSIONS AND RECOMMENDATIONS

This study has successfully demonstrated the feasibility of using chabazite columns to treat PWTW wastewater for  $^{137}\text{Cs}$  and/or  $^{90}\text{Sr}$ . This process has the potential of being a simple, economical process which will require much less operator attention than the present operations.

The study has also shown that the design of the columns is extremely important. Removal of all of the bed during sluicing is essential to the success of this process. The system must also be designed with adequate air-sparging and backwash capabilities to ensure long column life.

The data indicate that the columns are plugging before the chabazites have reached their sorption capacity. This may be partially due to inadequate prefiltration, algal or bacterial growth, physical degradation of the zeolite particles, or chemical reaction between the zeolite and feedwater. This area needs further investigation before full-scale columns are installed at the PWTW. Parameters which may effect plugging include type of chabazite, the flux across the column, pH of the feed, bed height, and prefiltration. However, economic analyses indicate that the chabazite system would be economical even if the plugging problems could not be eliminated.

Posttreatment processes need to be developed to reduce the leachability of zeolites that have been loaded with radionuclides. Open literature suggests that two approaches may be taken: (1) heat-treating to collapse the crystalline structure of the zeolites, thereby trapping the radionuclides; and (2) regenerating the zeolites with processes similar to those used with ion-exchange resin.

This study has also shown that traditional modeling techniques cannot be used to scale experimental data and design equipment for the chabazite systems. Fundamental studies are needed to develop models that could be used to design columns for maximum efficiency and that would eliminate extensive pilot-scale testing in the future. This type of model could result in significant cost savings in the future, as more waste streams require treatment and as disposal costs increase.

## 7. REFERENCES

1. E. D. Collins, J. M. Begovich, C. H. Brown, D. O. Campbell, L. C. Lasher, M. I. Morris, S. M. Robinson, and C. B. Scott, "An Improved Ion Exchange Method for Treatment of Slightly Contaminated Waste Waters," proceedings of American Nuclear Society International Meeting on Low-, Intermediate-, and High-Level Waste Management and Decontamination and Decommissioning, September 14-18, 1986.
2. J. B. Berry and S. M. Robinson, "Improved Treatment of Slightly Radioactive Waste - Reduced Generation of Wastes," proceedings of the Ninth Annual DOE Low-Level Waste Management Conference (in publication).
3. S. M. Robinson, J. M. Begovich, C. H. Brown, D. O. Campbell, and E. D. Collins, "Treatment of Radioactive Wastewaters By Chemical Precipitation and Ion Exchange," proceedings of the AIChE Spring National Meeting, Application of Adsorption and Ion Exchange Session, Symposium Series 5259, Houston, Texas, March 29-April 2, 1987.
4. S. M. Robinson and J. M. Begovich, Treatment Studies at the Process Waste Treatment Plant at Oak Ridge National Laboratory," ORNL/TM-10352 (in publication).
5. S. M. Robinson, Evaluation of Alternative Flowsheets for Upgrade of the Process Waste Treatment Plant," ORNL/TM-10576, (in publication).
6. A. K. Saha, P. Burn, D. K. Ploetz, D. C. Grant, and M. C. Skriba, "Design and Testing of Natural/Zeolite Ion Exchange Columns at West Valley," proceedings of the AIChE Spring National Meeting, Application of Adsorption and Ion Exchange Session, Symposium Series 5259, Houston, Texas, March 29-April 2, 1987.
7. S. L. Hoeffner, "Strontium Sorption on Savannah River Plant Soils," DP-1694, Savannah River Laboratory, Aiken, South Carolina, December 1984.
8. M. Howden and J. Pilot, "The Choice of Ion Exchanger for British Nuclear Fuels Ltd's Site Ion Exchange Effluent Plant," Ion Exchange Technology, Society of Chemical Industry, London, 1986, pp. 66-73.
9. E. D. Collins, D. O. Campbell, L. J. King, J. B. Knauer, and R. M. Wallace, "Development of the Flowsheet Used for Decontaminating High-Activity-Level Water," The Three Mile Island Accident, Diagnosis and Prognosis, ACS Symposium Series 293, American Chemical Society, Washington, DC, 1986, p. 212.

10. P. C. Wankat, Large-Scale Adsorption and Chromatography, Vol. 1, CRC Press, 1986.
11. M. D. LeVan and T. Vermeulen, "Channeling and Bed-Diameter Effects in Fixed-Bed Adsorber Performance," Adsorption and Ion Exchange - Progress and Future Prospects, AIChE Symposium Series, 80(233), 34 (1984).
12. M. S. Peters and K. D. Timmerhaus, Plant Design and Economics for Chemical Engineers, 2d ed., McGraw-Hill, St. Louis, 1968, pp. 175-83.
13. M. Lassiter, personal communication to S. M. Robinson, Engineering Division, Martin Marietta Energy Systems, Inc., Oak Ridge National Laboratory, December 1986.
14. H. K. S. Tan, "Programs for Fixed-Bed Sorption," Chem. Engr., 91,26 (December 24, 1984).
15. N. K. Hiester and T. Vermeulen, "Saturation Performance of Ion-Exchange and Adsorption Columns," Chem. Eng. Prog., 48, 505 (1952).
16. N. K. Hiester, T. Vermeulen, and G. Klein, Chemical Engineers' Handbook, Chap. 16, 6th ed., J. H. Perry, et al., eds., McGraw-Hill, New York, 1984.

8. APPENDIX

8.1 APPENDIX A. EXPERIMENTAL DATA

Table A.1. Breakthrough data for near-full-scale zeolite column

Date	FWTP feed		Zeolite effluent		Plant effluent		Cumulative volume processed (kgal)	Daily average flow (kgal)	Residence time (min)	Backwash date
	Gr. Beta (Bq/L)	<sup>137</sup> Cs (Bq/L)	Gr. Beta (Bq/L)	<sup>137</sup> Cs (Bq/L)	Gr. Beta (Bq/L)	<sup>137</sup> Cs (Bq/L)				
02/02					20	29	0	0		
02/03	1500	133	500	0	160	145	11	11		
02/04	1800	169	310	0	205	219	124	113	12.42	
02/12					247	217	150	26		
02/13	1900	154	340	0	75	89	258	108	13.00	
02/14					87	78	366	108	13.00	
02/15					33	25	490	124	11.32	
02/16					35		615	125	11.23	
02/17					36	0	731	116	12.10	
02/18	1700	161			61	43	837	106	13.25	
02/19	1800	107	690	12	154	77	943	106	13.25	
02/20					65	24	1062	119	11.80	
02/21					86	36	1165	103	13.63	
02/22					54	41	1271	106	13.25	
02/23					69	62	1362	91	15.43	
02/24					68	64	1461	99	14.18	
02/25	1800	138	1700	0	53	29	1571	110	12.76	
02/26					151	52	1687	116	12.10	
02/27					139	40	1805	118	11.90	
02/28					80	61	1916	111	12.65	
03/01					50	60	2036	120	11.70	
03/02					70	75	2152	116	12.10	
03/03					45	20	2260	108	13.00	
03/04	2000	156	1200	11	55	50	2370	110	12.76	
03/05					30	43	2471	101	13.90	
03/06					50	42	2586	115	12.21	
03/07					60	53	2687	101	13.90	
03/08					75	69	2793	106	13.25	
03/09					55	88	2887	94	14.94	
03/10					90	87	3005	118	11.90	
03/11	1600	172	1700	0	85	70	3124	119	11.80	
03/12					27	14	3238	114	12.32	
03/13					55	12	3348	110	12.76	
03/14					60	18	3454	106	13.25	
03/15					24	15	3568	114	12.32	
03/16					24	0	3690	122	11.51	
03/17					28	14	3815	125	11.23	
03/18	2000	237	730	0	18	13	3949	134	10.48	
03/19					22	16	4081	132	10.64	
03/20					22	14	4208	127	11.06	
03/21					28	11	4348	140	10.03	
03/22					23	20	4484	136	10.32	
03/23					30	12	4619	135	10.40	
03/24					25	0	4751	132	10.64	
03/25	1500	149	1500	12	24	12	4882	131	10.72	
03/26					78	0	5035	153	9.18	
03/27					24	16	5136	101	13.90	

Table A.1 (continued)

Date	FWTP feed		Zeolite effluent		Plant effluent		Cumulative volume processed (kgal)	Daily average flow (kgal)	Residence time (min)	Backwash date
	Gr. Beta (Bq/L)	<sup>137</sup> Cs (Bq/L)	Gr. Beta (Bq/L)	<sup>137</sup> Cs (Bq/L)	Gr. Beta (Bq/L)	<sup>137</sup> Cs (Bq/L)				
03/28					29	18	5237	101	13.90	
03/29					49	43	5338	101	13.90	
03/30					43	54	5440	102	13.76	
03/31					48	44	5551	111	12.65	
04/01	1900	156	1400	14	215	49	5672	121	11.60	
04/02					243	13	5786	114	12.32	
04/03					183	0	5910	124	11.32	
04/04					106	0	6013	103	13.63	
04/05					113	12	6113	100	14.04	
04/06					48	48	6220	107	13.12	
04/07					90	66	6324	104	13.50	
04/08	1700	149	1400	0	43	63	6455	131	10.72	
04/09					76	50	6584	129	10.88	
04/10					36	28	6718	134	10.48	
04/11					36	17	6848	130	10.80	
04/12					33	15	6977	129	10.88	
04/13					42	16	7103	126	11.14	
04/14					40	17	7226	123	11.41	
04/15	1200	226	1900	0	36	11	7303	77	18.23	
04/16					34	27	7344	41	34.24	
04/17					80	66	7379	35	40.11	
04/18					143	86	7422	43	32.65	
04/19					203	151	7481	59	23.80	
04/20					100	65	7585	104	13.50	
04/21	1300	162	1400	11	187	171	7689	104	13.50	
04/22	1600	172	1000	10	83	115	7793	104	13.50	
04/23					33	29	7896	103	13.63	
04/24					31		7982	86	16.33	
04/25					28		8063	81	17.33	
04/26					35		8149	86	16.33	
04/27					49	75	8259	110	12.76	
04/28					37	70	8332	73	19.23	
04/29	1200	121	1200	0	79	67	8381	49	28.55	
04/30					36	62	8461	80	17.55	
05/01					44		8562	101	13.90	
05/02					127		8644	82	17.12	
05/03					42		8644	0		
05/04					49		8737	93	15.10	
05/05					78		8834	97	14.47	
05/06	830	119		14	35		8903	69	20.35	
05/07					58		8984	81	17.33	
05/08					60		9073	89	15.78	
05/09					54		9160	87	16.14	
05/10					50		9248	88	15.95	
05/11					67		9297	49	28.65	
05/12					67		9406	109	12.88	
05/13	1600	179		15	103		9493	87	16.14	

Table A.1 (continued)

Date	<u>FWTP feed</u>		<u>Zeolite effluent</u>		<u>Plant effluent</u>		Cumulative volume processed (kgal)	Daily average flow (kgal)	Residence time (min)	Backwash date
	Gr. Beta (Bq/L)	<sup>137</sup> Cs (Bq/L)	Gr. Beta (Bq/L)	<sup>137</sup> Cs (Bq/L)	Gr. Beta (Bq/L)	<sup>137</sup> Cs (Bq/L)				
05/14					63		9584	91	15.43	
05/15					36	55	9679	95	14.78	
05/16					64	47	9762	83	16.92	
05/17					97	54	9836	74	18.97	
05/18					58	81	9912	76	18.47	
05/19					74	87	10058	146	9.62	
05/20	600	118	1000	16	116	91	10111	53	26.49	
05/21					27	14	10177	66	21.27	
05/22					51	67	10262	85	16.52	
05/23					84	86	10333	71	19.77	
05/24					86	90	10416	83	16.92	
05/25					57	79	10493	77	18.23	
05/26					39	42	10571	78	18.00	
05/27	1300	151	680	20	47	26	10645	74	18.97	
05/28					45	28	10712	67	20.96	
05/29					90	85	10775	63	22.29	
05/30					98	81	10835	60	23.40	
05/31					91	91	10902	67	20.96	
06/01					101	86	10966	64	21.94	
06/02					105	102	11028	62	22.65	
06/03	750	126	810	14	94	76	11086	58	24.21	
06/04					113	94	11150	64	21.94	
06/05					96	104	11202	52	27.00	
06/06					103	126	11259	57	24.63	
06/07					100	136	11314	55	25.53	
06/08					117	0	11377	63	22.29	
06/09					88	72	11398	21	66.86	
06/10	1000	304	1600	42	268	279	11486	88	15.95	
06/11					154	177	11577	91	15.43	
06/12					56	49	11640	63	22.29	
06/13					127	62	11683	43	32.65	
06/14					210	165	11715	32	43.88	
06/15					99	65	11738	23	61.04	
06/16					170	76	11761	23	61.04	
06/17	1300	179	590	14	230	150	11783	22	63.82	
06/18					270	212	11803	20	70.20	
06/19					390	242	11823	20	70.20	
06/20					57	21	11843	20	70.20	
06/21	680	276			31	22	11862	19	73.89	
06/22					25	31	11880	18	78.00	
07/01	1200	167	750	26	145	152	11966	84	16.71	06/30
07/02					160	124	12072	106	13.25	
07/03			450	15	170	98	12178	106	13.25	
07/04					76	112	12298	120	11.70	
07/05					113	98	12411	113	12.42	
07/06					56	67	12526	115	12.21	
07/07					57	53	12655	129	10.88	

Table A.1 (continued)

Date	WTP feed		Zeolite effluent		Plant effluent		Cumulative volume processed (kgal)	Daily average flow (kgal)	Residence time (min)	Backwash date
	Gr. Beta (Bq/L)	<sup>137</sup> Cs (Bq/L)	Gr. Beta (Bq/L)	<sup>137</sup> Cs (Bq/L)	Gr. Beta (Bq/L)	<sup>137</sup> Cs (Bq/L)				
07/08	1400	269			96	75	12758	103	13.63	
07/09					55	93	12875	117	12.00	
07/10					55	86	12980	105	13.37	
07/11					123	119	13099	119	11.80	
07/12					133	103	13217	118	11.90	
07/13					101	89	13354	137	10.25	
07/14					74	74	13488	134	10.48	
07/15	770	182	700	19	40	47	13617	129	10.88	
07/16					39		13751	134	10.48	
07/17					34	59	13867	116	12.10	
07/18					42	55	13969	102	13.76	
07/19					43	53	14070	101	13.90	
07/20					32	46	14174	104	13.50	
07/21					25	39	14273	99	14.18	
07/22	1100	151	570	22	72	34	14374	101	13.90	
07/23					42	39	14468	94	14.94	
07/24					46	40	14569	101	13.90	
07/25					30	35	14649	80	17.55	
07/26					89	83	14725	76	18.47	
07/27					86	88	14809	84	16.71	
07/28					82	74	14917	108	13.00	
07/29	1200	220	800	23	67	79	15022	105	13.37	
07/30					70	72	15125	103	13.63	
07/31					73	60	15245	120	11.70	
08/01					53	78	15333	88	15.95	
08/02					48	59	15416	83	16.92	
08/03					65	66	15491	75	18.72	
08/04					52	66	15567	76	18.47	
08/05	1200	181	1400	36	46	82	15622	55	25.53	
08/06					72	106	15669	47	29.87	
08/07					69	76	15748	79	17.77	
08/08					77	101	15823	75	18.72	
08/09					78	76	15936	113	12.42	
08/10					97	71	16041	105	13.37	
08/11					92	61	16096	55	25.53	
08/12	940	226	910	24	56	42	16146	50	28.08	
08/13					120	124	16221	75	18.72	
08/14					122	115	16292	71	19.77	
08/15					82	120	16369	77	18.23	
08/16					88	110	16429	60	23.40	
08/17					86	115	16491	62	22.65	
08/18					86	116	16550	59	23.80	08/18
08/19	1100	186	900	23	103	108	16616	66	21.27	
08/20					79	119	16701	85	16.52	
08/21					64	72	16799	98	14.33	
08/22					51	72	16890	91	15.43	
08/23					64	66	16997	107	13.12	

Table A.1 (continued)

Date	FWTP feed		Zeolite effluent		Plant effluent		Cumulative volume processed (kgal)	Daily average flow (kgal)	Residence time (min)	Backwash date
	Gr. Beta (Bq/L)	<sup>137</sup> Cs (Bq/L)	Gr. Beta (Bq/L)	<sup>137</sup> Cs (Bq/L)	Gr. Beta (Bq/L)	<sup>137</sup> Cs (Bq/L)				
08/24					38	50	17097	100	14.04	
08/25					37	45	17196	99	14.18	
08/26	1400	240	200	43	42	48	17298	102	13.76	
08/27					77	22	17380	82	17.12	
09/01					117	112	17465	85	16.52	
09/02	1300	160	150	39	97	129	17554	89	15.78	
09/03					90	137	17631	77	18.23	
09/04					53	52	17673	42	33.43	
09/05					41	42	17761	88	15.95	
09/06					82	101	17848	87	16.14	
09/07					116	94	17929	81	17.33	
09/08					113	111	18014	85	16.52	
09/09	1100	121	820	23	82	112	18100	86	16.33	
09/10					67	83	18180	80	17.55	
09/14					54	66	18656			09/11
09/15					60	77	18796	140	10.03	
09/16	1500	215	860	45	59	96	18935	139	10.10	
09/17					44	49	19076	141	9.96	
09/18					41	45	19214	138	10.17	
09/19					25	46	19330	116	12.10	
09/20					33	39	19433	103	13.63	
09/21					19	41	19537	104	13.50	
09/22					28	69	19619	82	17.12	
09/23	1200	144	440	78	30	109	19718	99	14.18	
09/24					34	85	19814	96	14.63	
09/25					54	76	19882	68	20.65	
09/26					34	61	19950	68	20.65	
09/27					39	52	20018	68	20.65	
09/28					33	44	20087	69	20.35	
09/29					37	50	20153	66	21.27	
09/30	1100		1300	264	22	34	20231	78	18.00	
10/01		267	830	26	36	35	20296	65	21.60	
10/02					48	81	20355	59	23.80	
10/03					103	106	20435	80	17.55	
10/04					88	100	20512	77	18.23	
10/05					75	93	20586	74	18.97	
10/06					59	60	20656	70	20.06	
10/07	1300	165	1200	28	40	41	20708	52	27.00	
10/08					51	37	20756	48	29.25	
10/09					52	78	20804	48	29.25	
10/10					69	84	20862	58	24.21	
10/11					62	92	20918	56	25.07	
10/12					50	84	20953	35	40.11	
10/13					48	67	21026	73	19.23	
10/14	1100		920	15	39	63	21085	59	23.80	
10/15					40	71	21142	57	24.63	
10/16					29	76	21197	55	25.53	

Table A.1 (continued)

Date	FWTP feed		Zeolite effluent		Plant effluent		Cumulative volume processed (kgal)	Daily average flow (kgal)	Residence time (min)	Backwash date
	Gr. Beta (Bq/L)	<sup>137</sup> Cs (Bq/L)	Gr. Beta (Bq/L)	<sup>137</sup> Cs (Bq/L)	Gr. Beta (Bq/L)	<sup>137</sup> Cs (Bq/L)				
10/17					54	74	21244	47	29.87	
10/18					51	72	21290	46	30.52	
10/19					47	68	21335	45	31.20	
10/20					30	76	21380	45	31.20	
10/21	1300		830	20	23	22	21417	37	37.95	
10/22					26	31	21455	38	36.95	
10/23					52	79	21490	35	40.11	
10/24					52	90	21524	34	41.29	
10/25					72	96	21554	30	46.80	
10/26					65	114	21569	15	93.60	
10/27					67	103	21582	13	108.00	
10/28	1400	207	980	22	78	106	21603	21	66.86	
10/29					84	111	21632	29	48.41	
10/30					100	164	21655	23	61.04	
10/31					77	102	21683	28	50.14	
11/01					75	123	21712	29	48.41	
11/02					78	112	21741	29	48.41	
11/03					84	117	21772	31	45.29	
11/04	1300	134	1300	32	80	116	21807	35	40.11	
11/05					89	140	21831	24	58.50	
11/06					47	55	21862	31	45.29	
11/07					20	12	21890	28	50.14	
11/08					38	55	21919	29	48.41	
11/09					56	83	21946	27	52.00	
11/10					57	92	21971	25	56.16	
11/11	1100	205	1200	34	52	106	21992	21	66.86	
11/12					72	129	22012	20	70.20	
11/13					123	173	22032	20	70.20	
11/14					105	149	22052	20	70.20	
11/15					66	118	22072	20	70.20	
11/16					105	117	22093	21	66.86	
11/17					46	47	22093	0	0.00	
11/18	1100	169			22	0	22093	0	0.00	
11/19					32	67	22093	0	0.00	
11/20					71	93	22093	0	0.00	
11/21					80	106	22093	0	0.00	
11/22					99	99	22093	0	0.00	
11/23					130	144	22093	0	0.00	
11/24					130	143	22105	12	117.00	
11/25					76	107	22173	68	20.65	
11/26					91	119	22237	64	21.94	
11/27					82	106	22301	64	21.94	
11/28					68	82	22358	57	24.63	
11/29					59	91	22413	55	25.53	
11/30					42	68	22464	51	27.53	
12/01					25	18	22513	49	28.65	
12/02	950	72		29	20	13				

Table A.2. Breakthrough data for pilot-scale zeolite columns

Date	Cycle number	Throughput (bed volumes)		Column influent values (Bq/L)												System effluent values (Bq/L)			Number of columns back-washed
		Total system	Lead column	1st column			2nd column			3rd Column			4th column			GB	Sr	Cs	
				GB	Sr	Cs	GB	Sr	Cs	GB	Sr	Cs	GB	Sr	Cs				
05/12	1	8406	118	1100	800		600	82		110	13		100	46		53	25		
05/13		8549	261	980	740		480	180		110	21		73	19		60	20		
05/14		8691	403	1100	860	186	58	19	0	38	1	0	55	17	0	120	16	0	
05/15		8842	554	960	560		65	22		33	1		48	10		42	13		
05/16		8989	701				72	23											
05/17		9127	839							23	1								
05/18		9258	970	956	690	130	48	25	0	31	1	0	32	13	0	29	7	0	
05/19		9404	1116	868	638		57	31		36	4		41	13		26	8		
05/20		9541	1253	771	530		75	59		45	5		47	13		25	7		
05/21		9864	1376	803	522	79	166	13	2	48	7	4	80	29	6	31	13	0	2
05/22		9771	1483	940	620		410	340		52	10		340	140		41	15		
05/23		9912	1624													45	13		
05/24		10032	1744													35	10		
05/25		10143	1855			121			0			0			0	33	10	0	
05/26		10239	1951	990	700		190	25		82	38		44	17		33	8		4
05/27		10344	2056	1000	750		260	190		76	25		50	10		34	8		
05/28		10477	2189	1000	790	111	230	190	0	42	16	12	30	8	0	35	6	0	
05/29		10602	2314	1000	710		250	180		68	27		40	11		25	6		1
05/30		10740	2452																
05/31		10888	2600																
06/01		11029	2741																
06/02		11184	2896	690	610	109	400	340	12	57	7	0	34	26	0	23	7	0	
06/03		11335	3047	830	760		430	390		63	30		28	9		26	8		
06/04		11474	3186	780	580	188	450	340	12	50	33	0	28	8	0	28	7	0	
06/05		11581	3293	850	790		520	440		79	45		40	10		32	10		1
06/06		11710	3422													37	11		
06/07		11847	3559													110	30		
06/08		11931	3643	1100	810	254	860	630	27	310	240	0	90	37	0	93	30	0	
06/09		11937	3649																1
06/24	2	12052	115	1100	960		320	240		41	25		94	34		53	31		
06/25		12205	268	1300	970		310	220		54	22		40	14		41	24		
06/26		12359	422	1300	730		280	180		59	20		42	11		46	14		
06/27		12511	574													41	14		
06/28		12666	729													43	12		
06/29		12820	883	1100	770		370	280		84	59		36	19		45	18		1
06/30		12968	1031	1000	790		340	290		150	56		33	16		87	17		
07/01		13108	1171	970	730		370	320		78	61		34	13		32	13		
07/02		13264	1327	970	630		30	260		75	54		30	13		42	12		
07/03		13418	1481													27	9		
07/04		13575	1638													27	9		
07/05		13729	1792													22	7		
07/06		13884	1947													23	8		
07/07		14039	2102	1200	760		380	280		110	58		40	9		61	7		2
07/08		14192	2255	1300	890		380	280		120	66		54	10		68	9		
07/09		14325	2388	1300	810		470	350		160	91		50	10		40	8		
07/10		14481	2544	1300	830		1500	1300		570	500		72	37		40	14		

Table A.2 (continued)

Date	Cycle number	Throughput (bed volumes)		Column influent values (Bq/L)												System effluent values (Bq/L)			Number of columns back-washed	
		Total system	Lead column	1st column			2nd column			3rd Column			4th column			GB	Sr	Cs		
				GB	Sr	Cs	GB	Sr	Cs	GB	Sr	Cs	GB	Sr	Cs					
07/11		14636	2699														49	19		
07/12		14793	2856														33	16		
07/13		14949	3012	1000	730	171	510	440	16	210	170	0	43	28	0	31	15	0		
07/14		15104	3167	950	690		540	440		220	170		44	27		33	13			
07/15		15259	3322	970	740		770	650		260	210		54	32		30	13			
07/16		15411	3474	990	970	151	730	730	13	250	240	0	63	42	0	26	17	0	1	
07/28	3	15598	139	790	650		380	300		89	34		56	14		81	31			
07/29		15751	292	900	440		380	140		93	36		46	8		49	12			
07/30		15902	443	800	650	163	360	300	0	80	44	0	39	16	0	41	19	0		
07/31		16058	599	750	550		330	250		79	26		37	15		34	11			
08/07	4	16245	145	840	560		120	90		50	25		56	25		47	0			
08/08		16401	301													41	20			
08/09		16558	458													48	18			
08/10		16716	616	1100	640	390	140	77	0	67	19	0	120	13	0	68	12	0		
08/11		16852	752	1100	750		130	85		74	29		44	10		99	13			
08/12		17008	908	1100	690		120	74		50	22		41	10		28	6			
08/13		17154	1054	1100	810	238	130	90	0	74	28	0	33	7	0	15	6	0		
08/14		17310	1210	1100	740		130	94		36	25		31	11		21	5			
08/15		17466	1366	1300	730		180	100		47	23		25	6		13	5			
08/16		17565	1465																	
08/21		17660	1560	1002	718		228	178		58	31		33	7		63	6			
08/22		17816	1716													22	6			
08/23		17970	1870													69	9			
08/24		18126	2026	1100	780	158	470	360	0	73	54	0	39	15	0	21	7	0		
08/25		18282	2182	970	630		430	320		74	47		36	13		33	7			
08/26		18436	2336	1100	720		480	390		98	60		38	13		32	7			
08/27		18591	2491	1000	720	148	530	420	0	150	100	0	54	21	0	31	8	0	1	
09/04	5	18706	115	960	850		120	73		54	22		76	24		22	1			
09/05		18855	264													14	1			
09/06		19013	422													16	1			
09/07		19165	574			158			0			0			0	11	1	0		
09/08		19317	726	1000	450		110	84		40	19		18	9		14	3			
09/09		19466	875	950	790		100	80		33	18		15	8		22	2			
09/10		19618	1027	880	660		96	65		38	18		23	6		25	2			
09/11		19769	1178	790	700		150	84		33	22		20	10		9	1		1	
09/12		19875	1284													8	1			
09/13		20031	1440													21	1			
09/14		20184	1593	1300	950	191	210	160	0	37	14	0	18	7	0	11	0	0		
09/15		20339	1748	1400	920		260	190		49	18		20	8		19	1			
09/16		20494	1903	1200	990		280	210		50	19		25	8		13	1			
09/17		20638	2047	1400	910	145	310	240	0	43	20	0	25	7	0	12	1	0	1	
09/18		20782	2191	1300	920		550	430		67	24		56	11		19	1			
09/19		20934	2343													19	2			
09/20		21089	2498													33	5			
09/21		21243	2652	1300	860	172	560	430	0	53	28	0	27	10	0	17	2	0		
09/22		21401	2810	1200	920		550	470		52	32		27	10		15	2			

Table A.2 (continued)

Date	Cycle number	Throughput (bed volumes)		Column influent values (Bq/L)												System effluent values (Bq/L)			Number of columns back-washed
		Total system	Lead column	1st column			2nd column			3rd Column			4th column			GB	Sr	Cs	
				GB	Sr	Cs	GB	Sr	Cs	GB	Sr	Cs	GB	Sr	Cs				
09/23		21555	2964	1200	880		840	690		130	99		50	21		22	3		1
09/24		21698	3107	1100	880		1100	870		150	110		44	26		18	7		1
09/30		21857	3266	1100	770		520	450		110	72		46	18		22	6		
10/01		22011	3420	1219	864		513	424		114	70		44	14		25	4		
10/03		22138	3547	1307	892		705	490											
10/04		22295	3704	1299	939		669	498											
10/05		22450	3859	1177	955		638	532		149	97		36	15		22	5		
10/06		22611	4000	1086	434		649	400		167	88		46	12		29	4		
11/06	6	22756	133	1100	870		360	260		63	23		41	6		23	3		
11/07		22910	287													25	4		
11/08		23065	442													28	6		
11/09		23220	597	1100	830	109	600	500	0	130	72	0	43	17	0	25	5	0	
11/10		23373	750	1100	610		500	330		120	59		52	14		32	3		

Table A.3. Pressure drops across pilot-scale zeolite columns

Date	Cycle number	Throughput (bed volumes)		Pressure drop across four columns (psi)				Number of columns back- washed
		Total system	Lead column	1st	2nd	3rd	4th	
05/12	1	8406	118	9	9	15	1	
05/13		8549	261	14	9	14	0	
05/14		8691	403	19	10	17	0	
05/15		8842	554	22	10	17	0	
05/16		8989	701	22	10	16	0	
05/17		9127	839	23	9	15	0	
05/18		9258	970	24	10	14	0	
05/19		9404	1116	30	12	22	0	
05/20		9541	1253	28	19	17	0	
05/21		9664	1376	22	20	18	0	2
05/22		9771	1483	4	4	26	4	
05/23		9912	1624	14	10	26	5	
05/24		10032	1744	30	12	21	4	
05/25		10143	1855	34	11	18	2	
05/26		10239	1951	38	7	15	0	4
05/27		10344	2056	28	5	8	0	
05/28		10477	2189	46	6	8	0	
05/29		10602	2314	52	5	9	0	1
05/30		10740	2452	17	6	9	0	
05/31		10888	2600	21	6	9	0	
06/01		11029	2741	25	7	8	0	
06/02		11184	2896	32	9	8	1	
06/03		11335	3047	37	9	9	1	
06/04		11474	3186	46	9	9	1	
06/05		11581	3293	51	10	8	1	1
06/06		11710	3422	28	18	10	0	
06/07		11847	3559	33	17	10	2	
06/08		11931	3643	32	30	11	1	
06/09		11937	3649					1
06/24	2	12052	115	8	12	0	5	
06/25		12205	268	10	16	2	5	
06/26		12359	422	16	19	5	5	
06/27		12511	574	31	27	8	4	
06/28		12666	729	21	18	6	4	
06/29		12820	883	23	28	6	4	1
06/30		12968	1031	8	23	5	5	
07/01		13108	1171	10	26	4	4	
07/02		13264	1327	12	26	4	4	
07/03		13418	1481	12	24	4	5	
07/04		13575	1638	14	23	6	4	
07/05		13729	1792	15	22	5	5	
07/06		13884	1947	16	25	5	5	
07/07		14039	2102	18	29	5	5	1
07/08		14192	2255	19	33	5	5	
07/09		14325	2388	11	33	6	5	
07/10		14481	2544	9	29	8	5	
07/11		14636	2699	9	27	7	6	

Table A.3 (continued)

Date	Cycle number	Throughput (bed volumes)		Pressure drop across four columns (psi)				Number of columns back- washed
		Total system	Lead column	1st	2nd	3rd	4th	
07/12		14793	2856	11	28	8	6	
07/13		14949	3012	10	26	7	6	
07/14		15104	3167	13	28	7	6	
07/15		15259	3322	14	26	8	7	
07/16		15411	3474	15	25	9	7	1
07/28	3	15598	139	12	7	4	4	
07/29		15751	292	14	8	3	4	
07/30		15902	443	12	10	3	4	
07/31		16058	599	14	10	3	4	
08/07	4	16245	145	20	2	2	4	
08/08		16401	301	21	2	2	4	
08/09		16558	458	21	3	1	5	
08/10		16716	616	20	3	1	5	
08/11		16852	752	22	3	1	4	
08/12		17008	908	22	3	1	4	
08/13		17154	1054	20	3	1	4	
08/14		17310	1210	19	3	2	4	
08/15		17466	1366	22	3	2	4	
08/16		17565	1465					
08/21		17660	1560	24	4	2	4	
08/22		17816	1716	26	3	3	3	
08/23		17970	1870	28	3	1	4	
08/24		18126	2026	31	3	2	4	
08/25		18282	2182	34	4	2	3	
08/26		18436	2336	33	4	2	4	
08/27		18591	2491	29	5	1	5	1
09/04	5	18706	115	12	10	6	0	
09/05		18855	264	12	8	6	0	
09/06		19013	422	17	10	6	0	
09/07		19165	574	19	10	6	0	
09/08		19317	726	21	9	6	0	
09/09		19466	875	24	8	6	0	
09/10		19618	1027	30	9	7	0	
09/11		19769	1178	40	10	6	0	1
09/12		19875	1284	17	23	6	0	
09/13		20031	1440	19	20	6	0	
09/14		20184	1593	21	19	6	0	
09/15		20339	1748	21	17	7	0	
09/16		20494	1903	24	17	7	0	
09/17		20638	2047	26	18	7	0	1
09/18		20782	2191	6	7	7	0	
09/19		20934	2343	10	10	7	0	
09/20		21089	2498	12	11	6	0	
09/21		21243	2652	14	10	7	0	
09/22		21401	2810	16	10	7	0	
09/23		21555	2964	9	18	8	0	1
09/24		21698	3107	5	14	8	0	1

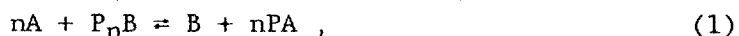
Table A.3 (continued)

Date	Cycle number	Throughput (bed volumes)		Pressure drop across four columns (psi)				Number of columns back- washed
		Total system	Lead column	1st	2nd	3rd	4th	
09/30		21857	3266	7	10	6	0	
10/01		22011	3420	8	10	7	0	
10/03		22138	3547	9	9	7	0	
10/04		22295	3704	10	11	7	0	
10/05		22450	3859	10	11	8	0	
10/06		22611	4020	10	12	7	0	
11/06	6	22756	133	15	7	6	0	
11/07		22910	287	17	7	7	0	
11/08		23065	442	18	7	7	0	
11/09		23220	597	18	7	8	0	
11/10		23373	750	17	7	6	0	

8.2 APPENDIX B. MODEL DEVELOPMENT

## 8.2 APPENDIX B. MODEL DEVELOPMENT

Thomas used experimental data to account for the equilibrium relationship, assumed a Langmuir isotherm, and approximated mass transfer by a second-order kinetic equation. Thomas assumed that the rate of adsorption of a single component on a resin can be represented by an expression suggested by the stoichiometry of the ion-exchange reaction



where A and B are the concentrations of the cations in the solution; PA and PB are the concentrations of the respective cations adsorbed on the resin, P; and n is the valence ratio of B to A. The concentration of A in the solution and resin at equilibrium is denoted by C and  $q^*$ , respectively. Assuming q and  $C_0$  are the total resin sites available and the total molar concentration in the solution, the second-order kinetic rate equation may be expressed as

$$\partial q^*/\partial t = K_a [C(q - q^*) - q^*/K_d(C_0 - C)], \quad (2)$$

where  $K_d$  is the equilibrium constant,  $K_a$  is the mass-transfer coefficient, and  $n = 1$ . The value of the mass-transfer coefficient is dependent on the controlling mechanism. For exchange of ions where  $n \neq 1$ , equivalent concentrations should be used instead of molar concentrations.

This equation can be normalized to obtain the general Thomas equation for the reaction kinetics of fixed-bed ion exchange:

$$-\frac{\partial X}{\partial N} \frac{1}{NT} = \frac{\partial Y}{\partial NT} \frac{1}{N} = X(1 - Y) - RY(1 - X), \quad (3)$$

where  $X$  and  $Y$  are the dimensionless concentrations of the solute ion in the fluid and solid phases, respectively; and  $R$  is the separation factor. The variable  $X$  is defined as  $C/C_0$ , and  $Y$  is defined as  $q^*/q$ . When the concentration of the solute ion is small relative to the concentration of the replaceable ion in the feed,  $R$  approaches unity and the isotherm is linear.

The variable  $N$  represents the length of the exchange column in transfer units and is defined by the expression

$$N = K_d' \rho_b K_a / (f/v) , \quad (4)$$

in which  $K_d'$  is the distribution coefficient when  $X = 1$ ,  $\rho_b$  is the bulk density of the ion exchanger,  $K_a$  is the mass-transfer coefficient characteristic of the system,  $f$  is the rate of flow of solution through the column, and  $v$  denotes the overall volume of the sorbent bed, including the void spaces. The throughput parameter,  $T$ , is defined to be

$$T = (V/v) / K_d' \rho_b , \quad (5)$$

where  $V$  is the volume of solution processed through the columns and  $V/v$  is the number of bed volumes of solution that has passed through the bed.

When  $\rho_b$  is constant, the volume-based distribution coefficient is defined as  $K_d = q_v/C_0$ , where  $q_v$  is the concentration of the solute ion per unit volume of sorbent bed (sorbent plus void space), and  $C_0$  is the concentration in the feed. Equations (4) and (5) can then be expressed as

$$N = K_d K_a / (f/v) , \quad (6)$$

and

$$T = (V/v)/K_d \quad (7)$$

When Eq. (3) is integrated for ion-exchange beds, assuming reversible second-order-reaction kinetics, the solution is:

$$X = C/C_0 = \frac{J(RN, NT)}{J(RN, NT) + [1 - J(N, RNT)] \exp[(R-1)N(T-1)]}, \quad (8)$$

and

$$Y = q/q^* = \frac{1 - J(RN, NT)}{J(RN, NT) + [1 - J(N, RNT)] \exp[(R-1)N(T-1)]}, \quad (9)$$

where  $J$  is a mathematical function related to the Bessel function.

Breakthrough curves are S-shaped curves obtained by plotting  $T$  (or  $V/v$ ) vs  $X$  on linear scales. Plotting these variables on logarithmic-probability scales eliminates the curvature of such plots and allows direct comparison with theoretical curves. The stoichiometric-equivalence point or "center of mass" is the value of  $X$  at  $T = 1$  for which the area below and to the left of the breakthrough curve equals the area above and to the right of the breakthrough curve. To a first approximation,  $X$  remains constant at this stoichiometric point. For large values of  $RN$ ,  $X \sim 0.5$  when  $T = 1$ .

In "trace systems," there is only one gross component. When one or more other components are present in such low concentrations that  $R$  approaches unity, the partial isotherm becomes linear. A useful definition of a trace system is that  $\Sigma x < 0.1$  and  $\Sigma y < 0.1$  for all solutes other than the gross component and also that  $R$  for the trace components must differ from unity by less than 0.1. Under these conditions, Eqs. (8) and (9) reduce to

$$X = J(N, NT) \quad (10)$$

and

$$Y = 1 - J(T, N) , \quad (11)$$

respectively.

Trace systems have the further property that, if more than one solute is present in low concentrations, each solute behaves as if the others were not present. The equilibrium and rate behavior of each trace component are effectively independent of the amounts and properties of other trace components. Therefore, all the dimensionless equations describing binary solutions can be extended to multicomponent systems by substituting the concentration of the component of interest for  $C$ ,  $q^*$ ,  $C_0$ , and  $q$ . These characteristics can be employed in data analysis. Experimental data can be used to construct breakthrough curves of  $X$  vs  $V/v$ . The value of  $K_d \approx$  to  $V/v$  where  $X \approx 0.5$ . Values for  $N$  can be obtained by comparing the experimental breakthrough curves (plotted on logarithmic-probability paper) with theoretical values available in many reference books.<sup>14-16</sup> For a trace system,  $R$  can be assumed to equal 1. The value of  $K_a$  can then be obtained from Eq. 6.

Once values of  $R$ ,  $N$ ,  $T$ , and  $K_a$  are obtained, these values can be used to predict the performance of columns at different operating conditions. The breakthrough curve at the new set of conditions will pass through the stoichiometric point, but the slope of the breakthrough curve will change. The slope of the new curve at each  $X$  value will be proportional to the slope at the central  $X$  point. This slope of the new curve is determined by the following two factors: (1) how  $N$  changes with the new conditions and (2) how the slope ratio changes with  $N$ .

It can be seen from Eq. (6) that the value of  $N$  will vary with  $K_a$ ,  $K_d$ ,  $v$ , and  $f$ . Vermeulen<sup>11</sup> developed equations to show how  $N$  changes for film and solid-diffusion-controlled mass transfer, respectively:

$$N = k_p z q / C_0 f [R - (R - 1)X], \quad (12)$$

and

$$N = k_f z / f [1 + (R - 1)X], \quad (13)$$

where  $k_p$ , the solid-diffusion-rate constant, is a function of the diffusion coefficient in the ion-exchange material and particle radius and  $k_f$ , the film-diffusion-rate coefficient, is a function of the diffusion coefficient in solution, the volumetric flow rate, and the particle radius. These equations have been reduced to

$$N \propto v S^{-a} f^{a-1} d^{a-2} D^{1-a}, \quad (14)$$

where  $S$  is the cross-sectional area of the column,  $d$  is the particle diameter, and  $D$  is the respective diffusion coefficient. Here  $a = 0$  for particle or pore diffusion, 0.5 for film diffusion, 1.0 for axial dispersion, and 2.0 for molecular diffusion.

If the controlling mass-transfer mechanism is known,  $N$  can be calculated from any reference  $N$  by taking the ratio of Eq. (14) with each set of conditions. If the flow rate and particle size remain constant,  $N$  varies proportionally with  $v$ . However, when the flow rate or particle size is also varied, the following proportionality applies:<sup>12</sup>

$$\frac{[T_x - 1]_{\text{pred}}}{[T_x - 1]_{\text{exp}}} = \frac{N_{\text{exp}}}{N_{\text{pred}}}^B, \quad (15)$$

where  $B$  depends on both  $R$  and  $N$  and is shown in Perry's model.

Perry's model states that when  $R = 1$ , the values for the mass transfer coefficient calculated for different controlling mechanisms are approximately equal.<sup>12</sup> Therefore,  $N$  is the same regardless of the controlling mechanism.

## INTERNAL DISTRIBUTION

- |                      |                               |
|----------------------|-------------------------------|
| 1. T. J. Abraham     | 37. T. E. Myrick              |
| 2. W. J. Armento     | 38. T. W. Oakes               |
| 3. P. T. Barton      | 39. J. R. Parrott             |
| 4. L. D. Bates       | 40-41. B. D. Patton           |
| 5. J. M. Begovich    | 42. C. E. Pepper              |
| 6. J. B. Berry       | 43. W. W. Pitt                |
| 7. C. H. Brown, Jr.  | 44. D. R. Reichle             |
| 8. D. O. Campbell    | 45. A. L. Rivera              |
| 9. R. M. Canon       | 46. S. M. Robinson            |
| 10. K. W. Cook       | 47. P. S. Rohwer              |
| 11. E. D. Collins    | 48. T. F. Scanlan             |
| 12. A. G. Croff      | 49. C. B. Scott               |
| 13. S. M. DePaoli    | 50. C. D. Scott               |
| 14. T. L. Donaldson  | 51. B. R. Reed                |
| 15. B. M. Eisenhower | 52. M. G. Stewart             |
| 16. S. B. Garland    | 53. L. H. Stinton             |
| 17. R. K. Genung     | 54. J. H. Swanks              |
| 18. R. W. Glass      | 55. P. A. Taylor              |
| 19. R. Hall          | 56. W. T. Thompson            |
| 20. R. J. Jolley     | 57. W. W. Thompson            |
| 21. J. R. Hightower  | 58. D. W. Turner              |
| 22. E. K. Johnson    | 59. V. L. Turner              |
| 23. J. M. Kennerly   | 60. V. C. A. Vaughen          |
| 24. C. M. Kendrick   | 61. A. B. Walker              |
| 25. T. M. Kent       | 62. J. F. Walker              |
| 26. L. C. Lasher     | 63. D. M. Walls               |
| 27. D. L. Lennon     | 64. J. S. Watson              |
| 28. J. J. Maddox     | 65. J. H. Wilson              |
| 29. R. C. Mason      | 66. K. Wilson                 |
| 30. C. P. McGinnis   | 67. Central Research Library  |
| 31. L. E. McGinnis   | 68. ORNL-Y-12 Tech. Library   |
| 32. L. E. McNeese    | Document Reference Section    |
| 33. C. Miller        | 69. Laboratory Records        |
| 34. M. E. Mitchell   | 70. Laboratory Records, ORNL- |
| 35. M. I. Morris     | 71. ORNL Patent Section       |
| 36. F. R. Mynatt     |                               |

## EXTERNAL DISTRIBUTION

72. R. W. Peters, Environmental Engineering, School of Civil Engineering, Purdue University, W. Lafayette, IN 47907
73. F. L. Culler, EPRI, 3412 Hillview Ave., Palo Alto, CA 94303
74. Director, Industrial Environmental Research Laboratory, U.S. Environmental Protection Agency, Cincinnati, OH 45268
75. Director, U.S. Environmental Protection Agency, Research Triangle Park, NC 27711
76. W. W. Eckenfelter, Jr., Vanderbilt University, Nashville, TN 37235
77. Office of Assistant Manager, Energy Research and Development, DOE-ORO, P.O. Box 2001, Oak Ridge, TN 37831

- 78-87. Office of Scientific and Technical Information, P.O. Box 62,  
Oak Ridge, TN 37831
88. Russell M. Propst, Duke Power Wachovia, P.O. Box 33189, Charlotte,  
NC 28242
89. Dennis Fennally, Union Carbide, 308 Harper Drive, Morristown, NJ  
08057
90. Neal J. Numark, ERR International, 3211 Germantown Road, Fairfax, VA  
22030
91. John G. Yates, USDOE, ER-42, Room 3F-091, Forrestal Bldg., 1000  
Independence Avenue, S.W., Washington, DC 20585
92. Ray Wilson, Steelhead Speciality Minerals, 1219 Washington Street,  
Suite 306, Spokane, WA 99201
93. Paul Highberger, 220 Stoneridge Drive, Columbia, SC 29210
94. Mike Harris, CH2M HILL, 800 Oak Ridge Turnpike, Jackson Plaza, C103,  
Oak Ridge, TN 37830
95. Sid du Mont, Chem. Nuc., 235 South Tulane Avenue, Oak Ridge, TN 37830
96. W. N. Lingle, DOE-ORO, P.O. Box 2001, Oak Ridge, TN 37831-8621
97. Louis Velazquez, DOE-ORO, P.O. Box 2001, Oak Ridge, TN 37831-8621
98. Doug Underwood, DOE-ORO, P.O. Box 2001, Oak Ridge, TN 37831-8621